



HAL
open science

Evaluation of the pathways of tropospheric nitrophenol formation using a multiphase model

M. A. J. Harrison, M. R. Heal, J. N. Cape

► **To cite this version:**

M. A. J. Harrison, M. R. Heal, J. N. Cape. Evaluation of the pathways of tropospheric nitrophenol formation using a multiphase model. *Atmospheric Chemistry and Physics Discussions*, 2005, 5 (2), pp.1115-1164. hal-00301038

HAL Id: hal-00301038

<https://hal.science/hal-00301038>

Submitted on 18 Jun 2008

HAL is a multi-disciplinary open access archive for the deposit and dissemination of scientific research documents, whether they are published or not. The documents may come from teaching and research institutions in France or abroad, or from public or private research centers.

L'archive ouverte pluridisciplinaire **HAL**, est destinée au dépôt et à la diffusion de documents scientifiques de niveau recherche, publiés ou non, émanant des établissements d'enseignement et de recherche français ou étrangers, des laboratoires publics ou privés.

**Pathways of
nitrophenol formation
using a multiphase
model**

M. R. Heal et al.

Evaluation of the pathways of tropospheric nitrophenol formation using a multiphase model

M. A. J. Harrison^{1,3}, M. R. Heal¹, and J. N. Cape²

¹School of Chemistry, University of Edinburgh, West Mains Road, Edinburgh EH9 3JJ, UK

²Edinburgh Research Station, Centre for Ecology and Hydrology, Bush Estate, Penicuik, Midlothian, EH26 0QB, UK

³current address: Hadley Centre, Met Office, FitzRoy Road, Exeter, EX1 3PB, UK

Received: 23 December 2004 – Accepted: 7 February 2005 – Published: 1 March 2005

Correspondence to: M. R. Heal (m.heal@ed.ac.uk)

© 2005 Author(s). This work is licensed under a Creative Commons License.

Title Page

Abstract

Introduction

Conclusions

References

Tables

Figures

⏪

⏩

◀

▶

Back

Close

Full Screen / Esc

Print Version

Interactive Discussion

EGU

Abstract

Phenols are a major class of volatile organic compounds (VOC) whose reaction within, and partitioning between, the gas and liquid phases affects their lifetime within the atmosphere, the local oxidising capacity, and the extent of production of nitrophenols, which are toxic chemicals. In this work, a zero-dimension box model was constructed to quantify the relative nitration pathways, and partitioning into the liquid phase, of mono-aromatic compounds in order to help elucidate the formation pathways of 2- and 4-nitrophenol in the troposphere. The liquid phase contributed significantly to the production of nitrophenols for liquid water content (L_c) values exceeding 3×10^{-9} , and for a range of assumed liquid droplet diameter, even though the resultant equilibrium partitioning to the liquid phase was much lower. For example, in a “typical” model scenario, with $L_c = 3 \times 10^{-7}$, 58% of nitrophenol production occurred in the liquid phase but only 2% of nitrophenol remained there, i.e. a significant proportion of nitrophenol observed in the gas phase may actually be produced via the liquid phase. The importance of the liquid phase was enhanced at lower temperatures, by a factor ~ 1.5 – 2 at 278 K cf. 298 K. The model showed that nitrophenol production was particularly sensitive to the values of the rate coefficients for the liquid phase reactions between phenol and OH or NO_3 reactions, but insensitive to the rate coefficient for the reaction between benzene and OH, thus identifying where further experimental data are required.

1. Introduction

Nitrophenols were first reported in the environment, in rainwater, by Nojima et al. (1975). Investigation of the potential sources of nitrophenols was stimulated by the suggestion that toxicity arising from the deposition of nitrophenols in rain could be one factor contributing to observed forest decline (Rippen et al., 1987; Natangelo et al., 1999). Subsequent analyses of samples of cloudwater, rainwater and snow have shown concentrations of nitrophenols to be significantly higher than would be expected

Pathways of nitrophenol formation using a multiphase model

M. R. Heal et al.

Title Page

Abstract

Introduction

Conclusions

References

Tables

Figures

⏪

⏩

◀

▶

Back

Close

Full Screen / Esc

Print Version

Interactive Discussion

**Pathways of
nitrophenol formation
using a multiphase
model**

M. R. Heal et al.

[Title Page](#)[Abstract](#)[Introduction](#)[Conclusions](#)[References](#)[Tables](#)[Figures](#)[◀](#)[▶](#)[◀](#)[▶](#)[Back](#)[Close](#)[Full Screen / Esc](#)[Print Version](#)[Interactive Discussion](#)

from their direct emission, e.g. (Levsen et al., 1990; Richartz et al., 1990; Tremp et al., 1993; Lüttke et al., 1997, 1999). Attention has therefore focused on the photochemical production of nitrophenols by reaction of mono-aromatics with OH radicals and NO_x present in the atmosphere (Harrison et al., 2005). These reactions can occur in the liquid or gas phases, or a combination of both. While pathways of gas-phase oxidation of benzene and alkylsubstituted benzenes have been extensively studied (Atkinson et al., 1992; Grosjean, 1991; Klotz et al., 1998; Knispel et al., 1990; Lay et al., 1996), the fate of these aromatics with respect to the aqueous phase is less well characterised.

Clouds are the most abundant form of condensed water in the troposphere covering around 60% of the earth at any one time. A moderately dense cloud has a volumetric liquid water content of only about 3×10^{-7} (Herterich and Herrmann, 1990; Molina et al., 1996), but despite the relatively sparse amounts of liquid water present in the atmosphere, condensed phase reactions play a surprisingly large role in atmospheric chemistry (Molina et al., 1996). One reason is the much larger rate coefficients for reactions occurring in the liquid phase.

The most abundant aromatic species in the atmosphere, such as toluene, xylene and benzene, have very low Henry's Law coefficients (expressed as a liquid to gas ratio) and consequently will not partition into the aqueous phase to any significant extent. This does not make the aqueous phase irrelevant, for two important reasons: first, the Henry's Law coefficient describes an equilibrium process but if liquid phase reaction is fast then the liquid phase may still act as a competitive reaction channel; secondly, the more polar phenolic and nitrophenolic products of mono-aromatic hydrocarbon oxidation are likely to have significantly higher solubility in atmospheric water (Harrison et al., 2002).

In this work a zero-dimensional box model was constructed to describe the essential features of the multiphase chemistry of the troposphere. The model was applied to identify the relative impact of different nitration pathways of mono-aromatics in the troposphere. It included the partitioning of 21 species and focused on the conversions of benzene to phenol to nitrophenols, in both the gas and liquid phases, and their phase

partitioning.

2. Description of the multiphase model

The zero-dimensional model was coded using the FACSIMILE software which is designed specifically to solve complex chemical mechanisms (FACSIMILE, 2001). The model incorporated emission, deposition, gas and liquid phase reactions and phase transfer. The kinetic, thermodynamic and initial-value data used in the model are listed in Tables A1–A19 of the Appendix, with brief descriptions given below.

2.1. Gas and liquid phase species and initial concentrations

Parameters describing the gas phase concentrations of species (Table A1) were taken from Herrmann et al. (1999, 2000) unless specified otherwise; time-dependent species were initialised with the values given in Table A2. All liquid phase species included in the mechanism (Table A3) were time-dependant, except for liquid water concentration H_2O , and were initialised with the values of Herrmann et al. (1999, 2000) unless specified otherwise.

2.2. Emissions

Source emission rates of certain species into the box (Table A4) were chosen such that the model would adequately simulate a typical polluted troposphere. The emission rates for benzene and NO were taken from the Chemical Mechanism Development (CMD) protocol as reported by Poppe et al. (2001). The emission of phenol was set at 1.5% the emission of benzene in accordance with data from the UK National Atmospheric Emissions Inventory (NAEI, 2002).

Pathways of nitrophenol formation using a multiphase model

M. R. Heal et al.

Title Page

Abstract

Introduction

Conclusions

References

Tables

Figures

⏪

⏩

◀

▶

Back

Close

Full Screen / Esc

Print Version

Interactive Discussion

Pathways of nitrophenol formation using a multiphase model

M. R. Heal et al.

Title Page

Abstract

Introduction

Conclusions

References

Tables

Figures

◀

▶

◀

▶

Back

Close

Full Screen / Esc

Print Version

Interactive Discussion

2.3. Dry deposition

The dry deposition velocities incorporated into the model are listed in Table A5. The deposition rate depends upon the value assigned to the depth of the boundary layer. In this model, an average depth of 1000 m was used. Since the dry deposition of O₃ and NO₂ are strongly linked to stomatal uptake, which in turn is related to the light intensity, this diurnal behaviour was incorporated by coding deposition velocity proportional to $J(\text{NO}_2)$.

2.4. Gas phase reactions

The latest IUPAC kinetic data were used to describe the “clean” inorganic gas phase reactions (Tables A6 and A7) with data from the latest Master Chemical Mechanism (as first described by Saunders et al., 1997) used for methane and aromatic gas phase reactions (Tables A8 to A9). Temperature dependent rate coefficients were explicitly coded using the appropriate Arrhenius expression data. Termolecular reaction rate coefficients were calculated from the parameters k_0 , k_∞ and F_c via the Troë approximation (Troë, 1983; Gilbert et al., 1983),

$$k = \frac{k_0 k_\infty F}{k_0 + k_\infty} \quad (1)$$

where F is defined by,

$$\log F = \frac{\log F_c}{1 + \left(\log \left(\frac{k_0}{k_\infty}\right)\right)^2} \quad (2)$$

2.5. Photolysis coefficients

Table A10 lists the gas phase photolysis reactions included in the model. The diurnal solar zenith angle χ was parameterised as described by Spencer (1971). “Clean”

chemistry photolysis rate coefficients were parameterised in terms of χ using the CMD data of Poppe et al. (2001),

$$J = A \exp \left(B \left(1 - \frac{1}{\cos(C\chi)} \right) \right) \quad (3)$$

whilst photolysis rate coefficients in gas phase methane oxidation were parameterised according to the MCM (Saunders et al., 1997),

$$J = A (\cos \chi)^B \exp(C \sec \chi) \quad (4)$$

(A , B and C are constants in each case).

2.6. Gas-liquid phase transfer

Clouds were modelled assuming monodisperse droplets of diameter, $d=1 \times 10^{-5}$ m. The “base scenario” cloud liquid volume fraction, L_c , was 3×10^{-7} . These values are in line with those used in other multiphase models (Herrmann et al., 2000; Lelieveld and Crutzen, 1990; Molina et al., 1996; Poppe et al., 2001) and are also in agreement with measured cloud data from Great Dun Fell in the UK (J. N. Cape, personal communication). However, given that the liquid water content of the atmosphere can vary widely (Voisin et al., 2000) the model was run for a range of L_c values.

Molecular phase transfer was treated using the approach of Schwartz (1986) in which the transfer rates from gas to liquid, and liquid to gas, are described by $\frac{1}{4} \bar{c} A_c \Gamma_{\text{overall}}$ and $\frac{\bar{c} A_c \Gamma_{\text{overall}}}{4 L_c H R T}$, respectively, where $\bar{c} = \sqrt{\frac{8RT}{\pi M}}$ is the mean molecular speed of the gas (M is the molar mass), R is the molar gas constant, T is the temperature, $A_c = \frac{6L_c}{d}$ is the specific surface area of the liquid phase, H is the Henry’s Law coefficient, and Γ_{overall} is the overall uptake coefficient. The latter was calculated via the equation,

$$\Gamma_{\text{overall}} = \frac{1}{\frac{\bar{c} d}{8D_g} - \frac{1}{2} + \frac{1}{\alpha}} \quad (5)$$

**Pathways of
nitrophenol formation
using a multiphase
model**

M. R. Heal et al.

Title Page

Abstract

Introduction

Conclusions

References

Tables

Figures

◀

▶

◀

▶

Back

Close

Full Screen / Esc

Print Version

Interactive Discussion

where, D_g is the gas phase diffusion coefficient and α is the mass accommodation coefficient.

The analysis assumes that species in the liquid phase are homogeneously dispersed throughout the entire droplet. This is justified as follows. The average distance travelled by diffusion in one dimension in time, t , is $\sqrt{2D_l t}$. For a typical liquid diffusion coefficient, D_l , of $1 \times 10^{-9} \text{ m}^2 \text{ s}^{-1}$ and droplet diameter of $1 \times 10^{-5} \text{ m}$, a species takes only 0.013 s on average to diffuse to the centre of a droplet.

The 21 species for which phase transfer was included are listed in Table A11. Unless otherwise specified, data for D_g , α and H were obtained from Herrmann et al. (1999, 2000). For species with no literature values of D_g , estimates were calculated using the method devised by Fuller et al. (1969).

2.7. Liquid phase reactions

As for the gas phase, the model included the liquid phase oxidation of organic compounds containing one carbon atom, as detailed in Tables A12 to A17. The majority of the reaction data were taken from Herrmann and co-workers (1999, 2000). Liquid phase photolysis rate coefficients were coded according to the CMD protocol (Poppe et al., 2001). Data for the aromatic chemistry in the liquid phase (Table A18) were taken from a number of sources. The rate coefficient for the reaction of benzene with OH was taken from Pan et al. (1993). For the reaction of phenol with NO_3 a value of $1.8 \times 10^9 \text{ L mol}^{-1} \text{ s}^{-1}$ was used (Barzagli and Herrmann, 2002) which compares well with the value of $1.9 \times 10^9 \text{ L mol}^{-1} \text{ s}^{-1}$ given in the UNARO report (UNARO, 2001). Rate data to describe the loss of phenol through reaction with OH were also taken from this latter report.

2.8. Reactions of aromatics

The degradation of aromatics in the troposphere is an area in which there remains a large amount of uncertainty. In this model, the benzene oxidation scheme shown

**Pathways of
nitrophenol formation
using a multiphase
model**

M. R. Heal et al.

Title Page

Abstract

Introduction

Conclusions

References

Tables

Figures

⏪

⏩

◀

▶

Back

Close

Full Screen / Esc

Print Version

Interactive Discussion

**Pathways of
nitrophenol formation
using a multiphase
model**

M. R. Heal et al.

[Title Page](#)[Abstract](#)[Introduction](#)[Conclusions](#)[References](#)[Tables](#)[Figures](#)[◀](#)[▶](#)[◀](#)[▶](#)[Back](#)[Close](#)[Full Screen / Esc](#)[Print Version](#)[Interactive Discussion](#)

in Fig. 1 was used, with data from version 3 of the MCM. Around 25% of the reaction of benzene with OH yields phenol, with the remaining products being ring-opened species. While the oxidation of benzene is also initiated by the NO₃ radical, this is only a minor route. The rate coefficient for the reaction of benzene with OH at 298 K is $1.39 \times 10^{-12} \text{ cm}^3 \text{ molecule}^{-1} \text{ s}^{-1}$ but $< 3 \times 10^{-17} \text{ cm}^3 \text{ molecule}^{-1} \text{ s}^{-1}$ for reaction with NO₃ (Calvert et al., 2002). Phenol reacts with OH and NO₃ via abstraction of the phenolic hydrogen to yield the C₆H₅O intermediate which may then combine with NO₂ to generate nitrophenol.

As indicated in Fig. 1, at each stage of this oxidation process the aromatic species may undergo phase transfer. Although benzene has a very small Henry's Law coefficient, those for phenol and nitrophenols are considerably greater. In the liquid phase, benzene is oxidised through reaction with OH to produce phenol as well as other liquid phase products. Oxidation of benzene may also be initiated by the NO₃ radical. The liquid phase rate coefficient of the reaction between NO₃ and benzene has been measured (Herrmann et al., 1995, 1996), but there have been no studies of the products of this reaction. The phenol present in the liquid may then react with NO₃ to yield nitrophenol, or may be lost from the system through reaction with OH. While the two isomers, 2-nitrophenol and 4-nitrophenol are thought to be the main reaction products of the reaction between phenol and NO₃, the proportion in which these species are produced under tropospherically-relevant conditions remains uncertain. Therefore in the model the ratio of the two nitrophenols formed was varied between the two different scenarios of predominantly 2NP production or predominantly 4NP production.

3. Results and discussion

The model was coded so that the different routes to formation of nitrophenol could be tracked. These routes are colour coded in the schematic in Fig. 2 and summarised with the nomenclature used here in Table 1. The same colour scheme is used in a number of the results graphs here. Liquid phase processes are defined as those in which there

**Pathways of
nitrophenol formation
using a multiphase
model**M. R. Heal et al.

[Title Page](#)[Abstract](#)[Introduction](#)[Conclusions](#)[References](#)[Tables](#)[Figures](#)[⏪](#)[⏩](#)[◀](#)[▶](#)[Back](#)[Close](#)[Full Screen / Esc](#)[Print Version](#)[Interactive Discussion](#)

has been a contribution from the liquid phase in the formation of the nitrophenols. These are represented by solid colours; the hatched colours signify the two gas phase only routes. The following additional abbreviations are used: NP2 and NP4 for 2- and 4-nitrophenol, respectively, present in the gas phase; and NP2L and NP4L for 2- and 4-nitrophenol present in the liquid phase. By comparing the route of formation with the final concentrations of the nitrophenols in each phase, it was possible to determine whether the nitrophenol produced in the gas phase was solely produced by gas phase reaction or whether liquid phase processes were involved.

3.1. Effect of the liquid phase

Figure 3 shows the modelled relative rate of total nitrophenol production through the various pathways at 278 K. As expected, the liquid phase becomes a more important route for the production of nitrophenols as the liquid water content is increased. For the driest scenario ($L_c=3\times 10^{-9}$), less than 2% of nitrophenol production is via liquid phase processes, increasing to over 93% under the wettest conditions modelled ($L_c=3\times 10^{-6}$). At the “benchmark” L_c value of 3×10^{-7} , 58% of nitrophenol production occurs via liquid phase processes. The model clearly shows that nitrophenol production is sensitive to realistic values of L_c . It is also apparent from Fig. 3 that the routes of nitrophenol production via oxidation of benzene to phenol in the liquid phase, LBLIQ and ABLIQ, are not significant at any value of L_c . This indicates that the low aqueous solubility of benzene is not sufficiently offset by fast aqueous phase reaction to compete with nitrophenol production via phenol.

Figure 4 shows how the nitrophenol generated by the routes illustrated in Fig. 3 is actually partitioned between the gas and liquid phases. The liquid phase product ratio for 2- and 4-nitrophenol is not known, and since the two nitrophenols have significantly different Henry’s Law values, the modelled atmospheric partitioning of these products depends sensitively on the assumed product ratio, as illustrated by Figs. 4a and b (for which 2-nitrophenol:4-nitrophenol product ratios of 90:10 and 10:90, respectively, were assumed). In each case, for the driest scenario, the nitration of phenol is

**Pathways of
nitrophenol formation
using a multiphase
model**

M. R. Heal et al.

[Title Page](#)[Abstract](#)[Introduction](#)[Conclusions](#)[References](#)[Tables](#)[Figures](#)[◀](#)[▶](#)[◀](#)[▶](#)[Back](#)[Close](#)[Full Screen / Esc](#)[Print Version](#)[Interactive Discussion](#)

dominated by the gas phase reaction path which only generates 2-nitrophenol. Since 2-nitrophenol has a relatively low Henry's Law coefficient (385 M atm^{-1} at 278 K) it remains almost exclusively in the gas phase. Figure 4a shows that even for the wetter scenarios, 2-nitrophenol remains the dominant product. This is a consequence of the dominance of 2-nitrophenol in the product ratio assumed in this scenario. The proportion of 4-nitrophenol is considerably greater in scenario Fig. 4b where, for an L_c value of 3×10^{-7} , 4-nitrophenol accounts for 52% of the total nitrophenol produced, reflecting the larger proportion of liquid phase reactions that generate 4-nitrophenol. However, while the relative amount of 2- or 4-nitrophenol has changed between these two scenarios, the total amount of nitrophenol partitioned into the liquid phase remains low; for $L_c = 3 \times 10^{-7}$ only 0.4% and 1.6% of nitrophenol is in the liquid phase for scenarios (a) and (b), respectively. Thus the key observation from comparison of Figs. 3 and 4 is that the contribution of the liquid phase to the production of nitrophenol (Fig. 3) is much larger than the fraction of nitrophenol that is observed in the liquid phase (Fig. 4). For example, when $L_c = 3 \times 10^{-7}$ the liquid phase accounts for 58% of the total rate of nitrophenol production but <2% of the nitrophenol distribution. This indicates that a considerable proportion of nitrophenol observed in the gas phase may actually be produced via liquid phase pathways and equilibrate into the gas phase.

3.2. Effect of temperature

Figures 5 and 6 show results for a temperature of 298 K. The rate of nitrophenol production was greater at 298 K (Fig. 5) than at 278 K (Fig. 3) over the whole range of L_c values. For example, for $L_c = 3 \times 10^{-7}$, nitrophenol production was almost 1.7 times greater at 298 K than at 278 K. On the other hand, the proportion of nitrophenol produced through liquid phase processes at $L_c = 3 \times 10^{-7}$ decreases from 58% at 278 K (Fig. 3) to 26% at 298 K (Fig. 5). The former observation is due to the general increase in reaction rates at higher temperature, while the latter observation is due to the reduction in aqueous solubility with temperature. (Note that such an interpretation is somewhat over-simplistic; multiphase tropospheric chemistry consists of many pro-

cesses affected differently by changes in temperature so whilst, for example, higher temperature may increase the rates of reactions from precursor to nitrophenol, it is likely also increase the rate of competing precursor loss processes.)

Figures 6a and b show that, at an L_c value of 3×10^{-7} , the proportion of nitrophenol actually partitioned in the liquid phase is only <0.1% and 0.2%, respectively. These proportions are lower than the equivalent proportions of 0.4% and 1.6% at 278 K (Fig. 4), despite the greater total production rate of nitrophenol at the higher temperature, because of the lower Henry's Law coefficients at higher temperatures. The reduced liquid phase nitrophenol production also affects the nitrophenol isomer ratio. At an L_c value of 3×10^{-7} , 4-nitrophenol comprises 6% and 52% of total nitrophenol produced at 278 K for scenarios (a) and (b), respectively, compared with 3% and 24% at 298 K.

Comparison of Figs. 5 and 6 again emphasises that a considerable proportion of nitrophenol ultimately partitioned in the gas phase may actually be formed in the liquid phase. For example, for $L_c = 3 \times 10^{-7}$, the liquid phase contributes 26% to total production of nitrophenol but $< \sim 0.2\%$ to the ultimate phase partitioning of the nitrophenol.

3.3. Sensitivity towards the liquid phase reaction rate coefficients

An important application of models is to investigate the sensitivity of output to variations in parameters whose values may be uncertain. One parameter for which laboratory data are sparse is the liquid phase reaction rate coefficient between benzene and OH. Although Figs. 3 and 6 suggest that this reaction is only a minor route in the production of nitrophenols, it is possible that a change to this rate coefficient might cause a large effect upon the system as a whole. However, simulations show that nitrophenol production at $L_c = 3 \times 10^{-7}$ is unaffected even when this rate coefficient is increased by two orders of magnitude. Only under the very wettest conditions is any nitrophenol formed via an increased rate of liquid phase reaction between benzene and OH, and even in this scenario this route contributes only 2.4% to nitrophenol production.

The effect of changing the rate coefficient for the reaction between phenol and NO_3

**Pathways of
nitrophenol formation
using a multiphase
model**

M. R. Heal et al.

Title Page

Abstract

Introduction

Conclusions

References

Tables

Figures

⏪

⏩

◀

▶

Back

Close

Full Screen / Esc

Print Version

Interactive Discussion

**Pathways of
nitrophenol formation
using a multiphase
model**

M. R. Heal et al.

[Title Page](#)[Abstract](#)[Introduction](#)[Conclusions](#)[References](#)[Tables](#)[Figures](#)[⏪](#)[⏩](#)[◀](#)[▶](#)[Back](#)[Close](#)[Full Screen / Esc](#)[Print Version](#)[Interactive Discussion](#)

to either $1.8 \times 10^8 \text{ L mol}^{-1} \text{ s}^{-1}$ or $1.8 \times 10^{10} \text{ L mol}^{-1} \text{ s}^{-1}$ is shown in Figs. 7a and b, respectively. The base scenario for comparison is Fig. 5, in which the value of the rate coefficient is $1.8 \times 10^9 \text{ L mol}^{-1} \text{ s}^{-1}$, as reported by Herrmann and co-workers (Barzaghi and Herrmann, 2002; Umschlag et al., 2002). When L_c is small ($< \sim 10^{-8}$), reactions in the liquid phase are not important, and changes to this rate coefficient have no impact on nitrophenol production. In contrast, for $L_c > \sim 10^{-8}$, comparison of Figs. 5 and 7 shows that an increase in phenol + NO_3 rate coefficient leads to a large increase in the amount of nitrophenol produced in the liquid phase, and vice versa. For $L_c = 3 \times 10^{-7}$, the proportion of nitrophenol produced in the liquid phase is 26% when the rate coefficient has the best-estimate value of $1.8 \times 10^9 \text{ L mol}^{-1} \text{ s}^{-1}$ (Fig. 5), but is 4% or 67% when the value of this rate coefficient is decreased, or increased, respectively, by an order of magnitude (Fig. 7).

Variation in the liquid phase phenol + NO_3 rate coefficient also impinges upon the amount of nitrophenol produced via the gas phase. This is because the liquid phase reaction between phenol and NO_3 also acts as an effective loss route for NO_3 , increasing the gas-to-liquid phase transfer of this radical and reducing its concentration in the gas phase. Figures 5 and 7b show that increasing the rate coefficient from $1.8 \times 10^9 \text{ L mol}^{-1} \text{ s}^{-1}$ to $1.8 \times 10^{10} \text{ L mol}^{-1} \text{ s}^{-1}$ for an L_c value of 3×10^{-7} reduces the amount of gas phase production of nitrophenol by $\sim 25\%$. This effect is likely further enhanced at lower temperatures (since lower temperatures also increase liquid phase transfer), although it would also depend on the degree of temperature dependence of the rate coefficient.

An equally important process is the reaction of phenol with OH which competes with the nitration reaction. The UNARO report (UNARO, 2001) gives a rate coefficient of $6.6 \times 10^9 \text{ L mol}^{-1} \text{ s}^{-1}$ for the phenol + OH reaction at 298 K, as used in the base scenario depicted in Fig. 5. Figures 8a and b show the effect of changing this rate coefficient value to $6.6 \times 10^8 \text{ L mol}^{-1} \text{ s}^{-1}$ and $6.6 \times 10^{10} \text{ L mol}^{-1} \text{ s}^{-1}$, respectively. As before, for liquid water content $< \sim 10^{-8}$, changes to the liquid phase reaction rate have little effect on production of nitrophenol. For higher values of liquid water content, a

higher value of the phenol + OH rate coefficient leads to less nitrophenol production. But changes in the rate of this reaction also give rise to changes in nitrophenol production in the gas phase (comparison of the hatched portions of Figs. 5 and 8). This is because the liquid phase reaction between phenol and OH also acts as a loss route for OH. Increasing the gas-to-liquid phase transfer of OH slows the rate of gas phase oxidation of benzene to phenol to nitrophenol, as illustrated in Fig. 1.

3.4. Effect of droplet diameter

As justified above, the base scenario droplet diameter was 1×10^{-5} m. Figures 9a and b show the effect of assuming that liquid water content was dispersed in droplets of diameter 1×10^{-4} m or 1×10^{-6} m, respectively. (Figure 5 is the comparative output for $d=1 \times 10^{-5}$ m at $T=298$ K.) From Figs. 5 and 9 the proportion of nitrophenol produced by liquid phase processes is 37, 26 and 5% when $d=1 \times 10^{-6}$, 1×10^{-5} and 1×10^{-4} m, respectively, for $L_c=3 \times 10^{-7}$. For a given L_c value, a smaller droplet diameter means a larger liquid phase specific area, A_c , which changes the phase-transfer kinetics because uptake coefficient, Γ_{overall} , is inversely proportional to d (Eq. 5). (Changing d at a given L_c does not change the equilibrium Henry's law phase partitioning, although larger droplets may reduce liquid phase mixing.)

Although a smaller droplet diameter increases the proportion of nitrophenol production in the liquid phase it decreases total nitrophenol production overall (Fig. 9b). As well as its direct impact on species that undergo phase transfer, a change in liquid phase specific area also indirectly impacts upon reactions of other species (in both phases) that do not undergo phase transfer. For example, when d is smaller, the gas phase concentrations of both OH and NO_3 are reduced, while in the liquid phase NO_3 is reduced but OH is increased. In the gas phase both OH and NO_3 affect both production and loss of nitrophenol, while in the liquid phase increased OH concentration limits nitrophenol production by removing phenol. As the effect of the liquid phase is enhanced at the smaller droplet size, this increase in liquid phase phenol + OH loss

Pathways of nitrophenol formation using a multiphase model

M. R. Heal et al.

Title Page

Abstract

Introduction

Conclusions

References

Tables

Figures

⏪

⏩

◀

▶

Back

Close

Full Screen / Esc

Print Version

Interactive Discussion

reaction has the overall effect of reducing the total amount of nitrophenol produced.

3.5. Comparison of model results with field observations

Model simulations of nitrophenol concentration were compared against the reported field data summarised in Table 2. Only general comparisons can be undertaken since the model was zero-dimensional and monodisperse and did not include emissions or concentration data specific to any particular field campaign.

The data presented in Figs. 3 to 9 are model simulations of two days, chosen to represent a reasonable air-mass processing time. The gas phase nitration of phenol is thought to yield mainly 2-nitrophenol so model simulations incorporating this as the dominant product of this reaction are most appropriate. Thus, the field data are compared in Table 2 with the model simulated data corresponding to Fig. 4a (i.e. best-guess base scenario, $T=278$ K). The model data are for $L_c=3\times 10^{-7}$ and have been converted to the appropriate units of ng m^{-3} and $\mu\text{g L}^{-1}$.

Table 2 shows that model simulated data are of an appropriate order of magnitude; for example, the value of 160 ng m^{-3} generated by the model for 2-nitrophenol in the gas phase is between the values of 350 ng m^{-3} measured at an urban site in Switzerland, and 24 ng m^{-3} measured at an urban site, in Oregon. The smaller concentrations of $0.8\text{--}6.4 \text{ ng m}^{-3}$ were measured at the remote site at Great Dun Fell (GDF). In addition to the atmospheric formation of nitrophenols by the routes indicated here, the observed data in Table 2 from urban areas may include nitrophenol emitted from primary sources such as car exhaust which is not considered in the model. Field measurements for 4-nitrophenol in the gas phase are only available from the GDF campaign ($1.2\text{--}35 \text{ ng m}^{-3}$) and from Rome ($\sim 22 \text{ ng m}^{-3}$). The model simulated concentrations (170 ng m^{-3}) are somewhat higher, although still reasonably consistent given that the model was not set up to simulate a particular real scenario.

At GDF, concentrations of 4-nitrophenol were generally higher than those for 2-nitrophenol (Table 2), whereas they are more similar for measurements in Rome and for the model data. The comparison is almost irrelevant because the model data relies

Pathways of nitrophenol formation using a multiphase model

M. R. Heal et al.

Title Page

Abstract

Introduction

Conclusions

References

Tables

Figures

⏪

⏩

◀

▶

Back

Close

Full Screen / Esc

Print Version

Interactive Discussion

on an assumption of 2-nitrophenol to 4-nitrophenol ratio.

Liquid phase nitrophenol measurements are available only for less polluted environments. Again the effect of the presumed pollution burden of the air mass can be seen with the values at Mount Brocken and the Vosges Mountains generally higher than those observed at the more remote site at GDF. Considering the lack of observational data at urban sites, the concentrations obtained by the model agree favourably with those values obtained by field work studies.

4. Conclusions

A box model of relevant multiphase tropospheric chemistry has shown that liquid water cloud/rain drops can contribute significantly to the formation of 2- and 4-nitrophenol from benzene and phenol emitted into the troposphere in the gas phase. The partitioning of nitrophenol product back into the gas phase often obscures the fact that a significant proportion of measured gas phase nitrophenol is produced through liquid phase reactions. The results emphasise the importance of ensuring that both liquid and gas phase processes are included for a complete understanding of the sources and fates of certain tropospheric species.

Acknowledgements. M. A. J. Harrison was supported by a studentship from the UK Engineering and Physical Sciences Research Council and CASE funding from the Centre for Ecology and Hydrology.

References

Atkinson, R., Aschmann, S. M., and Arey, J.: Reactions of OH and NO₃ radicals with phenol, cresols, and 2- nitrophenol at 296 K +/- 2 K, Environ. Sci. Technol., 26, 1397–1403, 1992.

Pathways of nitrophenol formation using a multiphase model

M. R. Heal et al.

Title Page

Abstract

Introduction

Conclusions

References

Tables

Figures

⏪

⏩

◀

▶

Back

Close

Full Screen / Esc

Print Version

Interactive Discussion

**Pathways of
nitrophenol formation
using a multiphase
model**

M. R. Heal et al.

[Title Page](#)[Abstract](#)[Introduction](#)[Conclusions](#)[References](#)[Tables](#)[Figures](#)[⏪](#)[⏩](#)[◀](#)[▶](#)[Back](#)[Close](#)[Full Screen / Esc](#)[Print Version](#)[Interactive Discussion](#)

- Barzaghi, P. and Herrmann, H.: A mechanistic study of the oxidation of phenol by OH/NO₂/NO₃ in aqueous solution, *Phys. Chem. Chem. Phys.*, 4, 3669–3675, 2002.
- Calvert, J. G., Atkinson, R., Becker, K. H., Kamens, R. M., Seinfeld, J. H., Wallington, T. J., and Yarwood, G.: The mechanisms of atmospheric oxidation of aromatic hydrocarbons, Oxford University Press, 2002.
- Cecinato, A., Di Palo, V., Pomata, D., Tomasi Sciano, M. C., and Possanzini, M.: Measurement of phase-distributed nitrophenols in Rome ambient air, *Chemosphere*, doi:10.1016/j.chemosphere.2004.10.045, 2005.
- FACSIMILE: FACSIMILE for Windows Version 3.0, MCPA Software Ltd., 2001.
- Finlayson-Pitts, B. J. and Pitts, J. N.: Chemistry of the upper and lower atmosphere: theory, experiments and applications, Academic Press, 2000.
- Fuller, E. D., Ensley, K., and Giddings, J. C.: Diffusion of halogenated hydrocarbons in helium, The effect of structure on collision cross sections, *J. Phys. Chem.*, 73, 3679–3685, 1969.
- Gilbert, R. G., Luther, K., and Troe, J.: Theory of Thermal Unimolecular Reactions in the Fall-Off Range, 2. Weak Collision Rate Constants, *Ber. Bunsenges. Phys. Chem.*, 87, 169–177, 1983.
- Grosjean, D.: Atmospheric fate of toxic aromatic compounds, *Sci. Total Environ.*, 100, 367–414, 1991.
- Harrison, M. A. J., Cape, J. N., and Heal, M. R.: Experimentally determined Henry's law coefficient of phenol, 2-methylphenol and 2-nitrophenol in the temperature range 281–302 K, *Atmos. Environ.*, 36, 1843–1851, 2002.
- Harrison, M. A. J., Barra, S., Borghesi, D., Vione, D., Arsene, C., and Iulian Olariu, R.: Nitrated phenols in the atmosphere: a review, *Atmos. Environ.*, 39, 231–248, 2005.
- Herrmann, H., Exner, M., Jacobi, H. W., Raabe, G., Reese, A., and Zellner, R.: Laboratory studies of atmospheric aqueous-phase free-radical chemistry: Kinetic and spectroscopic studies of reactions of NO₃ and SO₄⁻ radicals with aromatic compounds, *Faraday Discuss.*, 100, 129–153, 1995.
- Herrmann, H., Jacobi, H. W., Raabe, G., Reese, A., and Zellner, R.: Laser-spectroscopic laboratory studies of atmospheric aqueous phase free radical chemistry, *Fres. J. Anal. Chem.*, 355, 343–344, 1996.
- Herrmann, H., Ervens, B., Nowacki, P., Wolke, R., and Zellner, R.: A chemical aqueous phase radical mechanism for tropospheric chemistry, *Chemosphere*, 38, 1223–1232, 1999.
- Herrmann, H., Ervens, B., Jacobi, H. W., Wolke, R., Nowacki, P., and Zellner, R.: CAPRAM2.3:

**Pathways of
nitrophenol formation
using a multiphase
model**

M. R. Heal et al.

Title Page

Abstract

Introduction

Conclusions

References

Tables

Figures

◀

▶

◀

▶

Back

Close

Full Screen / Esc

Print Version

Interactive Discussion

A chemical aqueous phase radical mechanism for tropospheric chemistry, *J. Atmos. Chem.*, 36, 231–284, 2000.

Herterich, R. and Herrmann, R.: Comparing the distribution of nitrated phenols in the atmosphere of 2 german hill sites, *Environ. Technol.*, 11, 961–972, 1990.

5 Klotz, B., Barnes, I., and Becker, K. H.: New results on the atmospheric photooxidation of simple alkylbenzenes, *Chem. Phys.*, 231, 289–301, 1998.

Knispel, R., Koch, R., Siese, M., and Zetzsch, C.: Adduct formation of OH radicals with benzene, toluene, and phenol and consecutive reactions of the adducts with NO_x and O₂, *Ber. Bunsenges. Phys. Chem.*, 94, 1375–1379, 1990.

10 Lay, T. H., Bozzelli, J. W., and Seinfeld, J. H.: Atmospheric photochemical oxidation of benzene: Benzene + OH and the Benzene-OH adduct (Hydroxyl-2,4-cyclohexadienyl) + O₂, *J. Phys. Chem.*, 100, 6543–6554, 1996.

Lelieveld, J. and Crutzen, P. J.: Influences of cloud photochemical processes on tropospheric ozone, *Nature*, 343, 227–233, 1990.

15 Leuenberger, C., Ligocki, M. P., and Pankow, J. F.: Trace organic compounds in rain, 4. Identities, concentrations, and scavenging mechanisms for phenols in urban air and rain, *Environ. Sci. Technol.*, 19, 1053–1058, 1985.

Leuenberger, C., Czuczwa, J., Tremp, J., and Giger, W.: Nitrated phenols in rain: Atmospheric occurrence of phytotoxic pollutants, *Chemosphere*, 17, 511–515, 1988.

20 Levsen, K., Behnert, S., Prieß, B., Svoboda, M., Winkeler, H. D., and Zietlow, J.: Organic compounds in precipitation, *Chemosphere*, 21, 1037–1061, 1990.

Lüttke, J., Scheer, V., Levsen, K., Wunsch, G., Cape, J. N., Hargreaves, K. J., Storeton-West, R. L., Acker, K., Wieprecht, W., and Jones, B.: Occurrence and formation of nitrated phenols in and out of cloud, *Atmos. Environ.*, 31, 2637–2648, 1997.

25 Lüttke, J., Levsen, K., Acker, K., Wieprecht, W., and Möller, D.: Phenols and nitrated phenols in clouds at Mount Brocken, *Int. J. Environ. Anal. Chem.*, 74, 69–89, 1999.

Molina, M. J., Molina, L. T., and Kolb, C. E.: Gas-phase and heterogeneous chemical kinetics of the troposphere and stratosphere, *Ann. Rev. Phys. Chem.*, 47, 327–367, 1996.

NAEI: National Atmospheric Emissions Inventory, National Environmental Technology Centre, Abingdon, UK, <http://www.naei.org.uk>, 2002.

30 Natangelo, M., Mangiapan, S., Bagnati, R., Benfenati, E., and Fanelli, R.: Increased concentrations of nitrophenols in leaves from a damaged forestal site, *Chemosphere*, 38, 1495–1503, 1999.

**Pathways of
nitrophenol formation
using a multiphase
model**

M. R. Heal et al.

Title Page

Abstract

Introduction

Conclusions

References

Tables

Figures

◀

▶

◀

▶

Back

Close

Full Screen / Esc

Print Version

Interactive Discussion

Nojima, K., Fukaya, K., Fukui, S., and Kanno, S.: The formation of nitrophenols and nitrobenzene by the photochemical reaction of benzene in the presence of nitrogen monoxide, *Chemosphere*, 2, 77–82, 1975.

Pan, X. M., Schuchmann, M. N., and von Sonntag, C.: Oxidation of Benzene by the OH Radical – A Product and Pulse-Radiolysis Study in Oxygenated Aqueous-Solution, *J. Chem. Soc. Perkin Trans.*, 2, 289–297, 1993.

Poppe, D., Aumont, B., Ervens, B., Geiger, H., Herrmann, H., Roth, E. P., Seidl, W., Stockwell, W. R., Vogel, B., Wagner, S., and Weise, D.: Scenarios for modeling multiphase tropospheric chemistry, *J. Atmos. Chem.*, 40, 77–86, 2001.

Richartz, H., Reischl, A., Trautner, F., and Hutzinger, O.: Nitrated phenols in fog, *Atmos. Environ.*, 24, 3067–3071, 1990.

Rippen, G., Zietz, E., Frank, R., Knacker, T., and Klöpffer, W.: Do airborne nitrophenols contribute to forest decline?, *Environ. Technol. Lett.*, 8, 475–482, 1987.

Sander, R.: Compilation of Henry's Law Constants for Inorganic and Organic Species of Potential Importance in Environmental Chemistry (Version 3), <http://www.mpch-mainz.mpg.de/~sander/res/henry.html>, 1999.

Saunders, S. M., Jenkin, M. E., Derwent, R. G., and Pilling, M. J.: World Wide Web site of a Master Chemical Mechanism (MCM) for use in tropospheric chemistry models, *Atmos. Environ.*, 31, 1249–1249, 1997.

Schwartz, S. E.: Mass-transport considerations pertinent to aqueous phase reactions of gases in liquid-water clouds, in: *Chemistry of multiphase atmospheric systems*, edited by: Jaeschke, W., Springer Verlag, Berlin Heidelberg, 415–471, 1986.

Spencer, J. W.: Fourier series representation of the position of the sun, *Search*, 2, 172–173, 1971.

Tremp, J., Mattrel, P., Fingler, S., and Giger, W.: Phenols and nitrophenols as tropospheric pollutants – emissions from automobile exhausts and phase-transfer in the atmosphere, *Water Air Soil Pollut.*, 68, 113–123, 1993.

Troe, J.: Theory of Thermal Unimolecular Reactions in the Fall-Off Range, 1. Strong Collision Rate Constants, *Ber. Bunsenges. Phys. Chem.*, 87, 161–169, 1983.

Umschlag, T., Zellner, R., and Herrmann, H.: Laser-based studies of NO₃ radical reactions with selected aromatic compounds in aqueous solution, *Phys. Chem. Chem. Phys.*, 4, 2975–2982, 2002.

UNARO: Uptake and nitration of aromatics in the tropospheric atmosphere, Final report, EU

Environment Research Program contract No. ENV-4-CT-97-0411, 2001.
Voisin, D., Legrand, M., and Chaumerliac, N.: Scavenging of acidic gases (HCOOH, CH₃COOH, HNO₃, HCl, and SO₂) and ammonia in mixed liquid-solid water clouds at the Puy de Dome mountain (France), J. Geophys. Res., 105, 6817–6835, 2000.

ACPD

5, 1115–1164, 2005

**Pathways of
nitrophenol formation
using a multiphase
model**

M. R. Heal et al.

Title Page

Abstract

Introduction

Conclusions

References

Tables

Figures

⏪

⏩

◀

▶

Back

Close

Full Screen / Esc

Print Version

Interactive Discussion

EGU

Pathways of nitrophenol formation using a multiphase model

M. R. Heal et al.

Title Page

Abstract

Introduction

Conclusions

References

Tables

Figures

◀

▶

◀

▶

Back

Close

Full Screen / Esc

Print Version

Interactive Discussion

Table 1. Descriptions of the possible reaction pathways to nitrophenol formation with the associated colours and coding used in the figures.

Description of reaction pathway	Colour code in Fig. 2	Model code for product
Gas phase nitrophenol produced by gas phase reaction of phenol that was originally emitted into the gas phase	hatched blue	APH
Gas phase nitrophenol formed from gas phase phenol produced from benzene by gas phase reaction	hatched red	AB
Gas phase nitrophenol derived from gas phase phenol produced from benzene by liquid phase reaction	orange	ABLIQ
Liquid phase nitrophenol produced by the liquid phase reaction of phenol that was originally emitted into the gas but then partitioned into the liquid phase	green	LPH
Liquid phase nitrophenol formed from gas phase phenol produced from benzene by gas phase reaction	pink	LB
Liquid phase nitrophenol converted from liquid phase phenol produced from benzene by liquid phase reaction.	cyan	LBLIQ

Pathways of nitrophenol formation using a multiphase model

M. R. Heal et al.

Table 2. Measurements of 2- and 4-nitrophenol in cloudwater and the gas phase. Note that simultaneous measurement of concentrations in both phases has only been undertaken in the Great Dun Fell field campaign. Model simulation data correspond to Fig. 4a and are for two days at 278 K, with a volume fraction liquid water content of 3×10^{-7} , and assumed branching ratio for the reaction of phenol with NO_3 of 90% 2-nitrophenol and 10% 4-nitrophenol.

	Field observations		Model simulations (this study)	
	Gas phase / ng m^{-3}	Cloud / $\mu\text{g L}^{-1}$	Gas phase / ng m^{-3}	Cloud / $\mu\text{g L}^{-1}$
2-nitrophenol	0.8–6.4 ^a 24 ^b 350 ^d ~14 ^e	0.02–0.6 ^a 0.3 ^c	160 (6.9×10^8) ^g	1.4
4-nitrophenol	1.2–35 ^a ~22 ^e	0.05–4.9 ^a 1.7–16.3 ^f 21 ^c 5.4 ^c	170 (7.4×10^8) ^g	16

^a Great Dun Fell, England (Lüttke et al., 1997).

^b Portland, Oregon (Leuenberger et al., 1985).

^c Mount Brocken, Germany (Lüttke et al., 1999).

^d urban site, Switzerland (Leuenberger et al., 1988).

^e urban site, Rome, gas and particle-bound (Cecinato et al., 2005).

^f Vosges mountains, France (Levsen et al., 1990).

^g Values in parenthesis are gas phase concentrations in units of molecules cm^{-3} .

[Title Page](#)
[Abstract](#)
[Introduction](#)
[Conclusions](#)
[References](#)
[Tables](#)
[Figures](#)
[Back](#)
[Close](#)
[Full Screen / Esc](#)
[Print Version](#)
[Interactive Discussion](#)

Pathways of nitrophenol formation using a multiphase model

M. R. Heal et al.

Table A1. Concentrations of time-independent gas phase species.

Species	Concentration / molecules cm ⁻³
O ₂	5.1 × 10 ¹⁸
H ₂ O	5.1 × 10 ¹⁷
CO	5.1 × 10 ¹²
CH ₄	4.34 × 10 ¹³
CO ₂	9.5 × 10 ¹⁵
RH (alkane)	2.55 × 10 ¹¹
RO ₂ (alkyl peroxy radical)	3 × CH ₃ O ₂ ^a

^a estimated value to achieve a stable radical budget.

[Title Page](#)
[Abstract](#)
[Introduction](#)
[Conclusions](#)
[References](#)
[Tables](#)
[Figures](#)
[Back](#)
[Close](#)
[Full Screen / Esc](#)
[Print Version](#)
[Interactive Discussion](#)

Table A2. Initial concentrations of time-dependent gas phase species.

Variable	Initial concentration / molecules cm ⁻³
O ¹ D	5×10 ³
O ³ P	5×10 ³
N ₂ O	7.5×10 ¹²
CH ₃ NO ₃	6×10 ⁸
CH ₃ O ₂ NO ₂	1×10 ⁶
PH	2.55×10 ^{8a}
NO ₃	1.6×10 ^{7b}
BENZ	1.68×10 ^{11a}
OH	5×10 ³
HO ₂	5×10 ⁶
H ₂ O ₂	2×10 ^{10b}
HNO ₃	2.55×10 ^{10b}
HCHO	2×10 ^{8b}
HNO ₂	2×10 ⁸
HCOOH	2×10 ¹¹
CH ₃ O ₂	3×10 ⁸
CH ₃ OOH	2.55×10 ^{8b}
NO ₂	1.75×10 ^{10b}
N ₂ O ₅	5×10 ⁶
O ₃	5×10 ^{11b}
CH ₃ OH	1.275×10 ^{11b}
HO ₂ NO ₂	3×10 ⁷
NO	6×10 ⁹

^a (Leuenberger et al., 1988)^b (Herrmann et al., 1999, 2000)**Pathways of
nitrophenol formation
using a multiphase
model**

M. R. Heal et al.

Title Page

Abstract

Introduction

Conclusions

References

Tables

Figures

◀

▶

◀

▶

Back

Close

Full Screen / Esc

Print Version

Interactive Discussion

Table A3. Initial concentrations of time-dependent liquid phase species.

Variable	Starting concentration / moles L ⁻¹
H ⁺	3.16×10 ⁻⁵
OH ⁻	4×10 ⁻¹²
O ₂ ⁻	1×10 ⁻¹⁰
NO ₃ ⁻	1×10 ⁻¹⁰
NO ₂ ⁻	1×10 ⁻¹¹
O ₂ NO ₂ ⁻	1×10 ⁻¹⁰
H ₂ CO ₃	5×10 ⁻¹⁰
CO ₃ ²⁻	1×10 ⁻²²
CO ₃ ⁻	1×10 ⁻¹⁸
CH ₂ OHOH	4×10 ⁻⁵
HCOO ⁻	3×10 ⁻⁶
HCO ₃ ⁻	1×10 ⁻¹⁴
HOCl	1×10 ⁻¹⁰
Cl ₂	6×10 ⁻¹⁸
Cl ₂ ⁻	1×10 ⁻¹³
Cl	1×10 ⁻¹⁷
Cl ⁻	1×10 ⁻⁴
HCl	2×10 ⁻¹⁴
ClOH ⁻	1×10 ⁻¹⁷

^a (Leuenberger et al., 1988)

Pathways of nitrophenol formation using a multiphase model

M. R. Heal et al.

Title Page

Abstract

Introduction

Conclusions

References

Tables

Figures

◀

▶

◀

▶

Back

Close

Full Screen / Esc

Print Version

Interactive Discussion

Table A3. Continued.

Variable	Starting concentration / moles L ⁻¹
PH (phenol)	8.2×10^{-8a}
NO ₃	3.5×10^{-13}
BENZ (benzene)	6.1×10^{-9a}
OH	5×10^{-15}
HO ₂	1×10^{-9}
H ₂ O ₂	8×10^{-5}
HNO ₃	2.1×10^{-4}
HCHO	2×10^{-8}
HNO ₂	4×10^{-10}
HCOOH	5×10^{-5}
CH ₃ O ₂	7×10^{-12}
CH ₃ OOH	1×10^{-10}
NO ₂	8×10^{-12}
N ₂ O ₅	2.75×10^{-13}
O ₃	2×10^{-10}
CH ₃ OH	1×10^{-6}
CO ₂	1.1×10^{-5}
HO ₂ NO ₂	1×10^{-7}
NO	5×10^{-13}

^a (Leuenberger et al., 1988)

Pathways of nitrophenol formation using a multiphase model

M. R. Heal et al.

Title Page

Abstract

Introduction

Conclusions

References

Tables

Figures

◀

▶

◀

▶

Back

Close

Full Screen / Esc

Print Version

Interactive Discussion

**Pathways of
nitrophenol formation
using a multiphase
model**M. R. Heal et al.

Table A4. Emission rates of species introduced into the box model.

Species	Emission rate / molecules cm ⁻³ s ⁻¹
NO	2 × 10 ⁶
PH (phenol)	7.6 × 10 ²
BENZ (benzene)	5.1 × 10 ⁴

[Title Page](#)[Abstract](#)[Introduction](#)[Conclusions](#)[References](#)[Tables](#)[Figures](#)[I◀](#)[▶I](#)[◀](#)[▶](#)[Back](#)[Close](#)[Full Screen / Esc](#)[Print Version](#)[Interactive Discussion](#)

**Pathways of
nitrophenol formation
using a multiphase
model**M. R. Heal et al.

Table A5. Dry deposition velocities of species removed from the box model.

Species	Deposition rates / s^{-1}
H_2O_2	$5 \times 10^{-3}/1000$
HNO_3	$2 \times 10^{-2}/1000$
HNO_2	$5 \times 10^{-3}/1000$
O_3	$2 \times 10^{-3}/1000 + 1.089918 \times 10^{-3} \times J\text{NO}_2$
NO_2	$2.7248 \times 10^{-4} \times J\text{NO}_2$

[Title Page](#)[Abstract](#)[Introduction](#)[Conclusions](#)[References](#)[Tables](#)[Figures](#)[I◀](#)[▶I](#)[◀](#)[▶](#)[Back](#)[Close](#)[Full Screen / Esc](#)[Print Version](#)[Interactive Discussion](#)

Table A6. Reactions included in the “clean” chemistry of the gas phase and the corresponding rate coefficient expressions. ([M] is calculated for 1 atm pressure and model temperature.)

Reaction	Rate coefficient / cm ³ molecule ⁻¹ s ⁻¹
H ₂ O ₂ + OH → H ₂ O + HO ₂	2.9 × 10 ⁻¹² exp(-160/T)
NO + O ₃ → NO ₂	1.4 × 10 ⁻¹² exp(-1310/T)
O ¹ D → O ³ P	3.2 × 10 ⁻¹¹ exp(67/T) × [M]
O ₃ + OH → HO ₂	1.7 × 10 ⁻¹² exp(-940/T)
O ₃ + HO ₂ → OH	2.03 × 10 ⁻¹⁶ × (T/300) ^{4.57} exp(693/T)
NO + HO ₂ → NO ₂ + OH	3.6 × 10 ⁻¹² exp(270/T)
HO ₂ + HO ₂ → H ₂ O ₂	2.2 × 10 ⁻¹³ exp(600/T)
HO ₂ + HO ₂ → H ₂ O ₂	1.9 × 10 ⁻³³ × [M] exp(980/T)
NO ₂ + O ₃ → NO ₃	1.4 × 10 ⁻¹³ exp(-2470/T)
NO + NO ₃ → NO ₂ + NO ₂	1.8 × 10 ⁻¹¹ exp(110/T)
OH + HO ₂ → H ₂ O + O ₂	4.8 × 10 ⁻¹¹ exp(250/T)
OH + OH → H ₂ O + O ³ P	6.2 × 10 ⁻¹⁴ × (T/298) ^{2.6} exp(945/T)
O ³ P + O ₂ → O ₃	5.6 × 10 ⁻³⁴ × (T/300) ^{-2.8} × [M]
OH + HNO ₃ → H ₂ O + NO ₃	REUS1 + REUS2 where: REUS1 = 7.2 × 10 ⁻¹⁵ exp(785/T) REUS2 = (REUS3 × [M]) / (1 + (REUS3 × [M]) / REUS4) REUS3 = 1.9 × 10 ⁻³³ exp(725/T) REUS4 = 4.1 × 10 ⁻¹⁶ exp(1440/T)
CO + OH → H	1.3 × 10 ⁻¹³ × (1 + (0.6 × 300/T))
O ³ P + NO ₂ → NO	5.5 × 10 ⁻¹² exp(188/T)
OH + HO ₂ NO ₂ → NO ₂ ^a	1.3 × 10 ⁻¹² exp(380/T)
O ¹ D + N ₂ O → NO + NO	7.2 × 10 ⁻¹¹
O ¹ D + H ₂ O → OH + OH	2.2 × 10 ⁻¹⁰
OH + NO ₃ → HO ₂ + NO ₂	2 × 10 ⁻¹¹
OH + HNO ₂ → H ₂ O + NO ₂	2.5 × 10 ⁻¹² exp(260/T)
N ₂ O ₅ → HNO ₃ + HNO ₃	1 × 10 ⁻⁶

^a (Saunders et al., 1997)

**Pathways of
nitrophenol formation
using a multiphase
model**

M. R. Heal et al.

Title Page

Abstract

Introduction

Conclusions

References

Tables

Figures

◀

▶

◀

▶

Back

Close

Full Screen / Esc

Print Version

Interactive Discussion

Pathways of nitrophenol formation using a multiphase model

M. R. Heal et al.

Table A7. Termolecular reactions included in the “clean” chemistry of the gas phase and the data used to calculate the corresponding rate coefficient expressions^a.

Reaction	k_0	k_∞	F_C
$\text{OH} + \text{NO}_2 \rightarrow \text{HNO}_3$	$2.6 \times 10^{-30} \times (\text{T}/300)^{-2.9} \times [\text{M}]$	$7.5 \times 10^{-11} (\text{T}/300)^{-0.6}$	$\exp(-\text{T}/340)$
$\text{OH} + \text{OH} \rightarrow \text{H}_2\text{O}_2$	$6.9 \times 10^{-31} \times (\text{T}/300)^{-0.8} \times [\text{M}]$	2.6×10^{-11}	0.5
$\text{NO}_2 + \text{NO}_3 \rightarrow \text{N}_2\text{O}_5$	$2.8 \times 10^{-30} \times (\text{T}/300)^{-3.5} \times [\text{M}]$	$2 \times 10^{-12} (\text{T}/300)^{0.2}$	$2.5 \exp(-1950/\text{T})$ $+ 0.9 \exp(-\text{T}/430)$
$\text{N}_2\text{O}_5 \rightarrow \text{NO}_2 + \text{NO}_3$	$1 \times 10^{-3} \times (\text{T}/300)^{-3.5}$ $\exp(-11\,000/\text{T}) [\text{M}]$	$9.7 \times 10^{14} (\text{T}/300)^{0.1}$ $\exp(-11\,080/\text{T})$	$2.5 \exp(-1950/\text{T})$ $+ 0.9 \exp(-\text{T}/430)$
$\text{O}^3\text{P} + \text{NO}_2 \rightarrow \text{NO}_3$	$9 \times 10^{-32} \times (\text{T}/300)^{-2} \times [\text{M}]$	2.2×10^{-11}	$\exp(-\text{T}/1300)$
$\text{H} + \text{O}_2 \rightarrow \text{HO}_2$	$5.4 \times 10^{-32} \times (\text{T}/300)^{-1.8} \times [\text{M}]$	7.5×10^{-11}	$\exp(-\text{T}/498)$
$\text{O}^3\text{P} + \text{NO} \rightarrow \text{NO}_2$	$1 \times 10^{-31} \times (\text{T}/300)^{-1.6} \times [\text{M}]$	$3 \times 10^{-11} (\text{T}/300)^{0.3}$	$\exp(-\text{T}/1850)$
$\text{OH} + \text{NO} \rightarrow \text{HNO}_2$	$7.4 \times 10^{-31} \times (\text{T}/300)^{-2.4} \times [\text{M}]$	3.3×10^{-11}	$\exp(-\text{T}/1420)$
$\text{HO}_2 + \text{NO}_2 \rightarrow \text{HO}_2\text{NO}_2^b$	$1.80 \times 10^{-31} \times (\text{T}/300)^{-3.2} \times [\text{M}]$	4.70×10^{-12}	0.6
$\text{HO}_2\text{NO}_2 \rightarrow \text{HO}_2 + \text{NO}_2^b$	$4.10 \times 10^{-5} \exp(-10\,650/\text{T}) \times [\text{M}]$	5.70×10^{15} $\exp(-11\,170/\text{T})$	0.5

^a Rate coefficients are calculated from the data listed using the Troë formulation as described in the text.

^b (Saunders et al., 1997)

[Title Page](#)
[Abstract](#)
[Introduction](#)
[Conclusions](#)
[References](#)
[Tables](#)
[Figures](#)
[Back](#)
[Close](#)
[Full Screen / Esc](#)
[Print Version](#)
[Interactive Discussion](#)

Table A8. Reactions for the gas phase oxidation of methane and the corresponding rate coefficient expressions.

Reaction	Rate coefficient / cm ³ molecule ⁻¹ s ⁻¹ ^a		
OH + CH ₄ →CH ₃ O ₂	7.44 × 10 ⁻¹⁸ × T ² exp(-1361/T)		
CH ₃ O ₂ + HO ₂ →CH ₃ OOH	4.1 × 10 ⁻¹³ exp(790/T)		
OH + CH ₃ NO ₃ →HCHO + NO ₂	1.00 × 10 ⁻¹⁴ exp(1060/T)		
OH + CH ₃ OOH→CH ₃ O ₂	1.90 × 10 ⁻¹² exp(190/T)		
OH + CH ₃ OOH→HCHO + OH	1.00 × 10 ⁻¹² exp(190/T)		
CH ₃ O ₂ + NO→CH ₃ NO ₃	3.00 × 10 ⁻¹⁵ exp(280/T)		
CH ₃ O ₂ + NO→CH ₃ O + NO ₂	3.00 × 10 ⁻¹² exp(280/T)		
OH + HCHO→HO ₂ + CO	1.20 × 10 ⁻¹⁴ × T exp(287/T)		
CH ₃ OH + OH→HO ₂ + HCHO	6.01 × 10 ⁻¹⁸ × T ² exp(170/T)		
CH ₃ O ₂ →CH ₃ O	0.60 × 10 ⁻¹³ exp(416/T) × [CH ₃ O ₂]		
CH ₃ O ₂ →HCHO	0.61 × 10 ⁻¹³ exp(416/T) × [CH ₃ O ₂]		
CH ₃ O ₂ →CH ₃ OH	0.61 × 10 ⁻¹³ exp(416/T) × [CH ₃ O ₂]		
RH + OH→loss	5 × 10 ⁻¹³		
RH + NO ₃ →loss	1 × 10 ⁻¹⁵		
RO ₂ + NO→HO ₂ + NO ₂	3.00 × 10 ⁻¹² exp(280/T)		
CH ₃ O ₂ + NO ₃ →CH ₃ O + NO ₂	1 × 10 ⁻¹²		
NO ₃ + HCHO→HNO ₃ + CO + HO ₂	5.8 × 10 ⁻¹⁶		
CH ₃ O→HCHO + HO ₂	7.20 × 10 ⁻¹⁴ exp(-1080/T) × [M] × 0.2095		
	k ₀	k _∞	F _c
CH ₃ O ₂ + NO ₂ →CH ₃ O ₂ NO ₂	2.50 × 10 ⁻³⁰ × ((T/300) ^{-5.5}) × [M]	7.50 × 10 ⁻¹²	0.36
CH ₃ O ₂ NO ₂ →CH ₃ O ₂ + NO ₂	9.00 × 10 ⁻⁰⁵ exp(-9694/T) × [M]	1.10 × 10 ¹⁶ exp(-10561/T)	0.36

^a Rate coefficients for the last and penultimate reactions listed have units of s⁻¹ and cm⁶ molecule⁻² s⁻¹, respectively, and are calculated from the listed data using the Troë formulation as described in the text.

Pathways of nitrophenol formation using a multiphase model

M. R. Heal et al.

Title Page

Abstract

Introduction

Conclusions

References

Tables

Figures

◀

▶

◀

▶

Back

Close

Full Screen / Esc

Print Version

Interactive Discussion

Pathways of nitrophenol formation using a multiphase model

M. R. Heal et al.

Table A9. Gas phase reactions for the mono-aromatic species and corresponding rate coefficient expressions. (BENZ and PH represent benzene and phenol, respectively.)

Reaction	Rate coefficient / $\text{cm}^3 \text{ molecule}^{-1} \text{ s}^{-1}$
BENZ + OH → Ring Opened Species	$3.58 \times 10^{-12} \exp(-280/T) \times 0.65 \times 0.5$
BENZ + OH → Ring Opened Species + HO ₂	$3.58 \times 10^{-12} \exp(-280/T) \times 0.65 \times 0.5$
BENZ + OH → PH + HO ₂	$3.58 \times 10^{-12} \exp(-280/T) \times 0.25$
BENZ + OH → Ring Opened Species	$3.58 \times 10^{-12} \exp(-280/T) \times 0.10$
PH + OH → C ₆ H ₅ O	$2.63 \times 10^{-11} \times 0.067$
PH + OH → PH loss route	$2.63 \times 10^{-11} \times 0.933$
PH + NO ₃ → C ₆ H ₅ O + HNO ₃	$3.78 \times 10^{-12} \times 0.251$
PH + NO ₃ → PH loss route	$3.78 \times 10^{-12} \times 0.749$
C ₆ H ₅ O + NO ₂ → NITROPHENOL	3.90×10^{-13}

[Title Page](#)
[Abstract](#)
[Introduction](#)
[Conclusions](#)
[References](#)
[Tables](#)
[Figures](#)
[⏪](#)
[⏩](#)
[◀](#)
[▶](#)
[Back](#)
[Close](#)
[Full Screen / Esc](#)
[Print Version](#)
[Interactive Discussion](#)

Pathways of nitrophenol formation using a multiphase model

M. R. Heal et al.

Table A10. Gas phase photochemical reactions and the data used to parameterise the corresponding photochemical rate coefficients.

Reaction	A	B	C
$\text{NO}_2 \rightarrow \text{O}^3\text{P} + \text{NO}^{\text{a}}$	1.03×10^{-2}	9.61800×10^{-1}	8.46710×10^{-1}
$\text{O}_3 \rightarrow \text{O}^1\text{D}^{\text{a}}$	5.00×10^{-5}	3.29332	8.07820×10^{-1}
$\text{O}_3 \rightarrow \text{O}^3\text{P}^{\text{a}}$	5.11×10^{-4}	3.71950×10^{-1}	9.22890×10^{-1}
$\text{HNO}_2 \rightarrow \text{OH} + \text{NO}^{\text{a}}$	2.36×10^{-3}	1.06560	8.36440×10^{-1}
$\text{HNO}_3 \rightarrow \text{OH} + \text{NO}_2^{\text{a}}$	8.07×10^{-7}	2.30845	8.13640×10^{-1}
$\text{NO}_3 \rightarrow \text{NO}^{\text{a}}$	2.59×10^{-2}	2.96180×10^{-1}	9.37480×10^{-1}
$\text{NO}_3 \rightarrow \text{NO}_2 + \text{O}^3\text{P}^{\text{a}}$	2.30×10^{-1}	3.35180×10^{-1}	9.30590×10^{-1}
$\text{H}_2\text{O}_2 \rightarrow \text{OH} + \text{OH}^{\text{a}}$	1.18×10^{-5}	1.65050	8.16060×10^{-1}
$\text{HCHO} \rightarrow \text{CO} + \text{HO}_2 + \text{HO}_2^{\text{b}}$	4.642×10^{-5}	0.762	-0.353
$\text{HCHO} \rightarrow \text{CO} + \text{H}_2^{\text{b}}$	6.853×10^{-5}	0.477	-0.323
$\text{CH}_3\text{OOH} \rightarrow \text{CH}_3\text{O} + \text{OH}^{\text{b}}$	7.649×10^{-6}	0.682	-0.279
$\text{CH}_3\text{NO}_3 \rightarrow \text{CH}_3\text{O} + \text{NO}_2^{\text{b}}$	1.588×10^{-6}	1.154	-0.318

^a Photochemical rate coefficient parameterised using the formula of Poppe et al. (2001).

^b Photochemical rate coefficient parameterised using the formula of Saunders et al. (1997).

[Title Page](#)
[Abstract](#)
[Introduction](#)
[Conclusions](#)
[References](#)
[Tables](#)
[Figures](#)
[◀](#)
[▶](#)
[◀](#)
[▶](#)
[Back](#)
[Close](#)
[Full Screen / Esc](#)
[Print Version](#)
[Interactive Discussion](#)

Pathways of nitrophenol formation using a multiphase model

M. R. Heal et al.

Title Page

Abstract

Introduction

Conclusions

References

Tables

Figures

◀

▶

◀

▶

Back

Close

Full Screen / Esc

Print Version

Interactive Discussion

Table A11. Values of uptake parameters for species undergoing gas-liquid phase transfer. (NP2 and NP4 represent 2- and 4-nitrophenol, respectively.)

Species	$H / M \text{ atm}^{-1}$	α	$D_g / \text{cm}^2 \text{ s}^{-1}$	$\bar{c} / \text{cm s}^{-1}$
PH	$\exp((5850/T)-11.6)^a$	0.01^b	0.0853^c	25 908
NO ₃	0.6	4×10^{-3}	0.1	31 901
BENZ	$\exp((4000/T)-15.14)^d$	1×10^{-3b}	0.0895^c	28 441
OH	$25 \exp(5280 \times (1/T-1/298))$	0.05	0.153	60 922
HO ₂	9×10^3	0.01	0.104	43 726
H ₂ O ₂	$1 \times 10^5 \exp(6340 \times (1/T-1/298))$	0.11	0.146	43 078
HNO ₃	$2.1 \times 10^5 \exp(8700 \times (1/T-1/298))$	0.054	0.132	31 647
HCHO	$3000 \exp(7200 \times (1/T-1/298))$	0.02	0.164	45 860
HNO ₂	$49 \exp(4880 \times (1/T-1/298))$	0.5	0.13	36 639
HCOOH	$5 \times 10^3 \exp(5630 \times (1/T-1/298))$	0.012	0.153	37 035
CH ₃ O ₂	$6 \exp(5640 \times (1/T-1/298))$	3.8×10^{-3}	0.135	36 639
CH ₃ OOH	$6 \exp(5640 \times (1/T-1/298))$	3.8×10^{-3}	0.131	36 255
NO ₂	$1.2 \times 10^{-2} \exp(2500 \times (1/T-1/298))$	1.5×10^{-3}	0.192	37 035
N ₂ O ₅	1.4	3.7×10^{-3}	0.11	24 170
O ₃	$1.1 \times 10^{-2} \exp(2300 \times (1/T-1/298))$	5×10^{-2}	0.148	36 256
CH ₃ OH	$2.2 \times 10^2 \exp(5390 \times (1/T-1/298))$	1.5×10^{-2}	0.116	44 404
CO ₂	$3.1 \times 10^{-2} \exp(2423 \times (1/T-1/298))$	2×10^{-4}	0.155	37 868
HO ₂ NO ₂	1×10^5	0.1	0.13	28 261
NO	1.9×10^{-3}	0.01^e	0.227166^c	45 860
NP2	$\exp(6270/T-16.6)$	0.01	0.07727	21 305
NP4	$990 \times \exp(6000 \times (1/T-1/298))$	0.01	0.07727	21 305

^a (Harrison et al., 2002)

^b estimate

^c calculated values

^d obtained from the online database maintained by Sander (1999)

^e (Finlayson-Pitts and Pitts, 2000)

Pathways of nitrophenol formation using a multiphase model

M. R. Heal et al.

Table A12. Liquid phase OH reactions and the corresponding rate coefficient expressions.

Reaction	Rate coefficient / L mol ⁻¹ s ⁻¹
$O_3 + O_2^- + H^+ \rightarrow 2O_2 + OH$	$1.5 \times 10^9 / H^+$
$HO_2 + HO_2 \rightarrow O_2 + H_2O_2$	$8.3 \times 10^5 \exp(-2720 \times (1/T - 1/298))$
$HO_2 + O_2^- + H^+ \rightarrow H_2O_2 + O_2$	$9.7 \times 10^7 \exp(-1060 \times (1/T - 1/298)) / H^+$
$HO_2 + OH \rightarrow H_2O + O_2$	1×10^{10}
$O_2^- + OH \rightarrow OH^- + O_2$	$1.1 \times 10^{10} \exp(-2120 \times (1/T - 1/298))$
$H_2O_2 + OH \rightarrow HO_2 + H_2O$	$3 \times 10^7 \exp(-1680 \times (1/T - 1/298))$
$CH_3OOH + OH \rightarrow CH_3O_2 + H_2O$	$3 \times 10^7 \exp(-1680 \times (1/T - 1/298))$

Title Page

Abstract

Introduction

Conclusions

References

Tables

Figures

◀

▶

◀

▶

Back

Close

Full Screen / Esc

Print Version

Interactive Discussion

Pathways of nitrophenol formation using a multiphase model

M. R. Heal et al.

[Title Page](#)
[Abstract](#)
[Introduction](#)
[Conclusions](#)
[References](#)
[Tables](#)
[Figures](#)
[◀](#)
[▶](#)
[◀](#)
[▶](#)
[Back](#)
[Close](#)
[Full Screen / Esc](#)
[Print Version](#)
[Interactive Discussion](#)

Table A13. Liquid phase nitrogen-species reactions and the corresponding rate coefficient expressions.

Reaction	Rate coefficient / L mol ⁻¹ s ⁻¹
$\text{N}_2\text{O}_5 + \text{H}_2\text{O} \rightarrow \text{H}^+ + \text{H}^+ + \text{NO}_3^- + \text{NO}_3^-$	$5 \times 10^9 \exp(-1800 \times (1/T - 1/298))$
$\text{NO}_3 + \text{OH}^- \rightarrow \text{NO}_3^- + \text{OH}$	$9.4 \times 10^7 \exp(-2700 \times (1/T - 1/298))$
$\text{NO}_3 + \text{H}_2\text{O}_2 \rightarrow \text{NO}_3^- + \text{H}^+ + \text{HO}_2$	$4.9 \times 10^6 \exp(-2000 \times (1/T - 1/298))$
$\text{NO}_3 + \text{CH}_3\text{OOH} \rightarrow \text{NO}_3^- + \text{H}^+ + \text{CH}_3\text{O}_2$	$4.9 \times 10^6 \exp(-2000 \times (1/T - 1/298))$
$\text{NO}_3 + \text{HO}_2 \rightarrow \text{NO}_3^- + \text{H}^+ + \text{O}_2$	3×10^9
$\text{NO}_3 + \text{O}_2^- \rightarrow \text{NO}_3^- + \text{O}_2$	3×10^9
$\text{NO}_2 + \text{OH} \rightarrow \text{NO}_3^- + \text{H}^+$	1.2×10^{10}
$\text{NO}_2 + \text{O}_2^- \rightarrow \text{NO}_2^- + \text{O}_2$	1×10^8
$\text{NO}_2 + \text{NO}_2 \rightarrow \text{HNO}_2 + \text{NO}_3^- + \text{H}^+$	$1 \times 10^8 \exp(2900 \times (1/T - 1/298))$
$\text{O}_2\text{NO}_2^- \rightarrow \text{NO}_2^- + \text{O}_2$	4.5×10^{-2}
$\text{NO}_2^- + \text{OH} \rightarrow \text{NO}_2 + \text{OH}^-$	1.1×10^{10}
$\text{NO}_2^- + \text{NO}_3 \rightarrow \text{NO}_3^- + \text{NO}_2$	1.4×10^9
$\text{NO}_2^- + \text{Cl}_2^- \rightarrow \text{Cl}^- + \text{Cl}^- + \text{NO}_2$	6×10^7
$\text{NO}_2^- + \text{CO}_3^- \rightarrow \text{CO}_3^{2-} + \text{NO}_2$	$6.6 \times 10^5 \exp(-850 \times (1/T - 1/298))$
$\text{NO}_2^- + \text{O}_3 \rightarrow \text{NO}_3^- + \text{O}_2$	$5 \times 10^5 \exp(-6900 \times (1/T - 1/298))$
$\text{HNO}_2 + \text{OH} \rightarrow \text{NO}_2 + \text{H}_2\text{O}$	1×10^9

Pathways of nitrophenol formation using a multiphase model

M. R. Heal et al.

Table A14. Liquid phase organic reactions and the corresponding rate coefficient expressions.

Reaction	Rate coefficient / L mol ⁻¹ s ⁻¹
CH ₃ OH + OH → H ₂ O + HO ₂ + HCHO	1 × 10 ⁹ exp(-580 × (1/T - 1/298))
CH ₃ OH + NO ₃ → NO ₃ ⁻ + H ⁺ + HO ₂ + HCHO	5.4 × 10 ⁵ exp(-4300 × (1/T - 1/298))
CH ₃ OH + Cl ₂ ⁻ → 2Cl ⁻ + H ⁺ + HO ₂ + HCHO	1000 exp(-5500 × (1/T - 1/298))
CH ₃ OH + CO ₃ ⁻ → CO ₃ ²⁻ + H ⁺ + HO ₂ + HCHO	2.6 × 10 ³
CH ₂ (OH) ₂ + OH → H ₂ O + HO ₂ + HCOOH	1 × 10 ⁹ exp(-1020 × (1/T - 1/298))
CH ₂ (OH) ₂ + NO ₃ → NO ₃ ⁻ + H ⁺ + HO ₂ + HCOOH	1 × 10 ⁶ exp(-4500 × (1/T - 1/298))
CH ₂ (OH) ₂ + Cl ₂ ⁻ → Cl ⁻ + Cl ⁻ + H ⁺ + HO ₂ + HCOOH	3.1 × 10 ⁴ exp(-4400 × (1/T - 1/298))
CH ₂ (OH) ₂ + CO ₃ ⁻ → CO ₃ ²⁻ + H ⁺ + HO ₂ + HCOOH	1.3 × 10 ⁴
HCOOH + OH → H ₂ O + HO ₂ + CO ₂	1.3 × 10 ⁸ exp(-1000 × (1/T - 1/298))
HCOO ⁻ + OH → OH ⁻ + HO ₂ + CO ₂	4 × 10 ⁹ exp(-1020 × (1/T - 1/298))
HCOOH + NO ₃ → NO ₃ ⁻ + H ⁺ + HO ₂ + CO ₂	3.8 × 10 ⁵ exp(-3400 × (1/T - 1/298))
HCOO ⁻ + NO ₃ → NO ₃ ⁻ + HO ₂ + CO ₂	5.1 × 10 ⁷ exp(-2200 × (1/T - 1/298))
HCOOH + Cl ₂ ⁻ → 2Cl ⁻ + H ⁺ + HO ₂ + CO ₂	5500 exp(-4500 × (1/T - 1/298))
HCOO ⁻ + Cl ₂ ⁻ → Cl ⁻ + Cl ⁻ + HO ₂ + CO ₂	1.3 × 10 ⁶
HCOO ⁻ + CO ₃ ⁻ → CO ₃ ²⁻ + HO ₂ + CO ₂	1.4 × 10 ⁵ exp(-3300 × (1/T - 1/298))
CH ₃ O ₂ + CH ₃ O ₂ → CH ₃ OH + HCHO + O ₂	1.7 × 10 ⁸ exp(-2200 × (1/T - 1/298))

Title Page

Abstract

Introduction

Conclusions

References

Tables

Figures

⏪

⏩

◀

▶

Back

Close

Full Screen / Esc

Print Version

Interactive Discussion

Pathways of nitrophenol formation using a multiphase model

M. R. Heal et al.

Table A15. Liquid phase chlorine-species reactions and their corresponding rate coefficient expressions.

Reaction	Rate coefficient / $\text{L mol}^{-1} \text{s}^{-1}$
$\text{NO}_3 + \text{Cl}^- \rightarrow \text{NO}_3^- + \text{Cl}$	$1 \times 10^7 \exp(-4300 \times (1/T - 1/298))$
$\text{Cl}_2^- + \text{Cl}_2 \rightarrow \text{Cl}_2 + 2\text{Cl}^-$	8.7×10^8
$\text{Cl}_2^- + \text{H}_2\text{O}_2 \rightarrow \text{Cl}^- + \text{Cl}^- + \text{H}^+ + \text{HO}_2$	$7 \times 10^5 \exp(-3340 \times (1/T - 1/298))$
$\text{Cl}_2^- + \text{CH}_3\text{OOH} \rightarrow \text{Cl}^- + \text{Cl}^- + \text{H}^+ + \text{CH}_3\text{O}_2$	$7 \times 10^5 \exp(-3340 \times (1/T - 1/298))$
$\text{Cl}_2^- + \text{OH}^- \rightarrow \text{Cl}^- + \text{Cl}^- + \text{OH}$	4×10^6
$\text{Cl}_2^- + \text{HO}_2 \rightarrow \text{Cl}^- + \text{Cl}^- + \text{H}^+ + \text{O}_2$	1.3×10^{10}
$\text{Cl}_2^- + \text{O}_2^- \rightarrow 2\text{Cl}^- + \text{O}_2$	6×10^9
$\text{Cl}_2 + \text{H}_2\text{O} \rightarrow \text{H}^+ + \text{Cl}^- + \text{HOCl}$	$0.40 \exp(-7900 \times (1/T - 1/298))$

[Title Page](#)
[Abstract](#)
[Introduction](#)
[Conclusions](#)
[References](#)
[Tables](#)
[Figures](#)
[⏪](#)
[⏩](#)
[◀](#)
[▶](#)
[Back](#)
[Close](#)
[Full Screen / Esc](#)
[Print Version](#)
[Interactive Discussion](#)

Pathways of nitrophenol formation using a multiphase model

M. R. Heal et al.

Table A16. Liquid phase carbonate reactions and their corresponding rate coefficient expressions.

Reaction	Rate coefficient / L mol ⁻¹ s ⁻¹
$\text{HCO}_3^- + \text{OH}^- \rightarrow \text{H}_2\text{O} + \text{CO}_3^-$	$1.7 \times 10^7 \exp(-1900 \times (1/T - 1/298))$
$\text{CO}_3^{2-} + \text{OH}^- \rightarrow \text{OH}^- + \text{CO}_3^-$	$1 \times 10^9 \exp(-2550 \times (1/T - 1/298))$
$\text{CO}_3^{2-} + \text{NO}_3^- \rightarrow \text{NO}_3^- + \text{CO}_3^-$	1.7×10^7
$\text{CO}_3^{2-} + \text{Cl}_2^- \rightarrow 2\text{Cl}^- + \text{CO}_3^-$	2.7×10^6
$\text{CO}_3^- + \text{CO}_3^- \rightarrow 2\text{O}_2^- + 2\text{CO}_2$	2.2×10^6
$\text{CO}_3^- + \text{H}_2\text{O}_2 \rightarrow \text{HCO}_3^- + \text{HO}_2$	4.3×10^5
$\text{CO}_3^- + \text{CH}_3\text{OOH} \rightarrow \text{HCO}_3^- + \text{CH}_3\text{O}_2$	4.3×10^5
$\text{CO}_3^- + \text{HO}_2 \rightarrow \text{HCO}_3^- + \text{O}_2$	6.5×10^8
$\text{CO}_3^- + \text{O}_2^- \rightarrow \text{CO}_3^{2-} + \text{O}_2$	6.5×10^8

[Title Page](#)
[Abstract](#)
[Introduction](#)
[Conclusions](#)
[References](#)
[Tables](#)
[Figures](#)
[⏪](#)
[⏩](#)
[◀](#)
[▶](#)
[Back](#)
[Close](#)
[Full Screen / Esc](#)
[Print Version](#)
[Interactive Discussion](#)

Pathways of nitrophenol formation using a multiphase model

M. R. Heal et al.

[Title Page](#)
[Abstract](#)
[Introduction](#)
[Conclusions](#)
[References](#)
[Tables](#)
[Figures](#)
[◀](#)
[▶](#)
[◀](#)
[▶](#)
[Back](#)
[Close](#)
[Full Screen / Esc](#)
[Print Version](#)
[Interactive Discussion](#)
Table A17. Liquid phase equilibria and the corresponding rate coefficient expressions.

Reaction	Forward rate coefficient / L mol ⁻¹ s ⁻¹	Backward rate coefficient / L mol ⁻¹ s ⁻¹
H ₂ O = H ⁺ + OH ⁻	2.34 × 10 ⁻⁵ exp(-6800 × (1/T-1/298))	1.3 × 10 ¹¹
CO ₂ + H ₂ O = H ₂ CO ₃	4.3 × 10 ⁻² exp(-9250 × (1/T-1/298))	5.6 × 10 ⁴ exp(-8500 × (1/T-1/298))
H ₂ CO ₃ = H ⁺ + HCO ₃ ⁻	1 × 10 ⁷	5 × 10 ¹⁰
HCO ₃ ⁻ = H ⁺ + CO ₃ ²⁻	2.35 exp(-1820 × (1/T-1/298))	5 × 10 ¹⁰
HO ₂ = H ⁺ + O ₂ ⁻	8 × 10 ⁵	5 × 10 ¹⁰
HNO ₃ = H ⁺ + NO ₃ ⁻	1.1 × 10 ¹² exp(1800 × (1/T-1/298))	5 × 10 ¹⁰
HNO ₂ = H ⁺ + NO ₂ ⁻	2.65 × 10 ⁷ exp(-1760 × (1/T-1/298))	5 × 10 ¹⁰
HO ₂ NO ₂ = H ⁺ + O ₂ NO ₂ ⁻	5 × 10 ⁵	5 × 10 ¹⁰
NO ₂ + HO ₂ = HO ₂ NO ₂	1 × 10 ⁷	4.6 × 10 ⁻³
HCOOH = HCOO ⁻ + H ⁺	8.85 × 10 ⁶ exp(12 × (1/T-1/298))	5 × 10 ¹⁰
HCHO + H ₂ O = CH ₂ (OH) ₂	0.18 exp(4030 × (1/T-1/298))	5.1 × 10 ⁻³
Cl + Cl ⁻ = Cl ₂ ⁻	2.7 × 10 ¹⁰	1.4 × 10 ⁵
Cl ⁻ + OH = ClOH ⁻	4.3 × 10 ⁹	6.1 × 10 ⁹
ClOH ⁻ + H ⁺ = Cl + H ₂ O	2.1 × 10 ¹⁰	1.3 × 10 ³
ClOH ⁻ + Cl ⁻ = Cl ₂ ⁻ + OH ⁻	1 × 10 ⁴	4.5 × 10 ⁷
HCl = H ⁺ + Cl ⁻	8.6 × 10 ¹⁶ exp(6890 × (1/T-1/298))	5 × 10 ¹⁰

**Pathways of
nitrophenol formation
using a multiphase
model**M. R. Heal et al.

Table A18. Liquid phase mono-aromatic reactions and the corresponding rate coefficient expressions. (BENZ and PH represent benzene and phenol, respectively.)

Reaction	Rate coefficient / $\text{L mol}^{-1} \text{s}^{-1}$
BENZ + OH → PH	1.55×10^8
BENZ + OH → Other products	1.55×10^8
PH + OH → PH loss route	6.6×10^9
PH + NO ₃ → NITROPHENOL	1.8×10^9

[Title Page](#)[Abstract](#)[Introduction](#)[Conclusions](#)[References](#)[Tables](#)[Figures](#)[I◀](#)[▶I](#)[◀](#)[▶](#)[Back](#)[Close](#)[Full Screen / Esc](#)[Print Version](#)[Interactive Discussion](#)

Pathways of nitrophenol formation using a multiphase model

M. R. Heal et al.

Table A19. Liquid phase photochemical reactions included in the model, together with the constants used to parameterise the corresponding photochemical rate coefficients.

Reaction ^a	A	B	C
$\text{H}_2\text{O}_2 \rightarrow \text{OH} + \text{OH}$	1.359×10^{-5}	1.449	1.007
$\text{NO}_2^- \rightarrow \text{NO} + \text{OH} + \text{OH}^-$	8.757×10^{-5}	1.343	9.156×10^{-1}
$\text{NO}_3^- \rightarrow \text{NO}_2 + \text{OH} + \text{OH}^-$	1.439×10^{-6}	1.480	1.019

^a Photochemical rate coefficient parameterised using the formula of Poppe et al. (2001).

Title Page

Abstract

Introduction

Conclusions

References

Tables

Figures

◀

▶

◀

▶

Back

Close

Full Screen / Esc

Print Version

Interactive Discussion

Pathways of nitrophenol formation using a multiphase model

M. R. Heal et al.

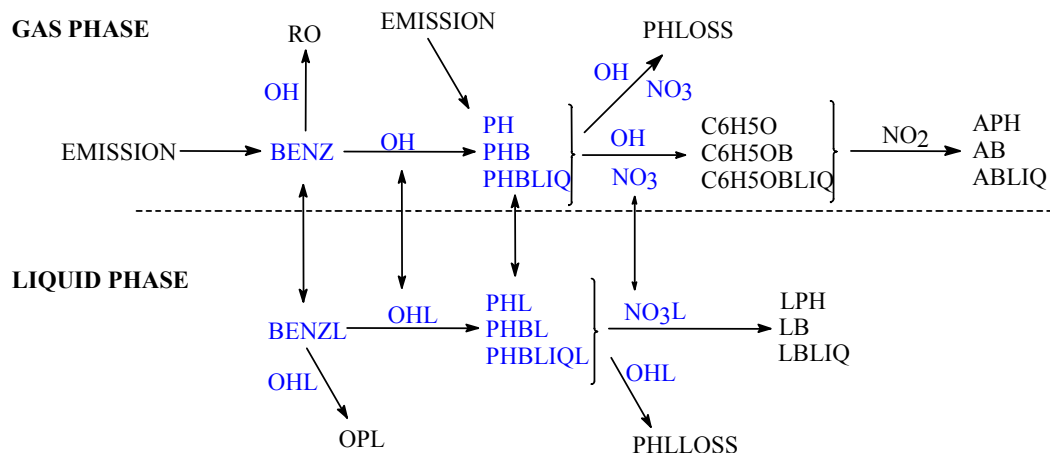


Fig. 1. Schematic of the aromatic chemistry in both the gas and liquid phases. Double headed arrows represent phase transfer between the gas and the liquid phase. The terms APH, AB, ABLIQ, LPH, LB, LBLIQ all refer to nitrophenol product but formed through different reaction paths through the scheme, as described in Table 1 and illustrated in Fig. 2.

Title Page

Abstract

Introduction

Conclusions

References

Tables

Figures

◀

▶

◀

▶

Back

Close

Full Screen / Esc

Print Version

Interactive Discussion

Pathways of nitrophenol formation using a multiphase model

M. R. Heal et al.

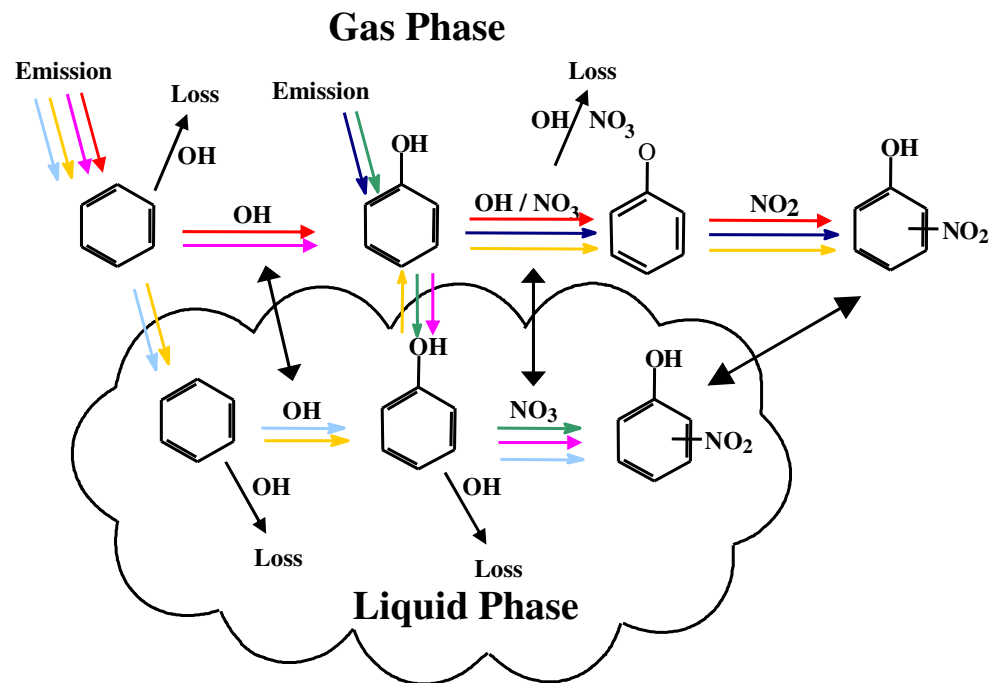


Fig. 2. Schematic of the colour scheme used to describe each different reaction path to nitrophenol formation.

Title Page

Abstract

Introduction

Conclusions

References

Tables

Figures

◀

▶

◀

▶

Back

Close

Full Screen / Esc

Print Version

Interactive Discussion

EGU

Pathways of nitrophenol formation using a multiphase model

M. R. Heal et al.

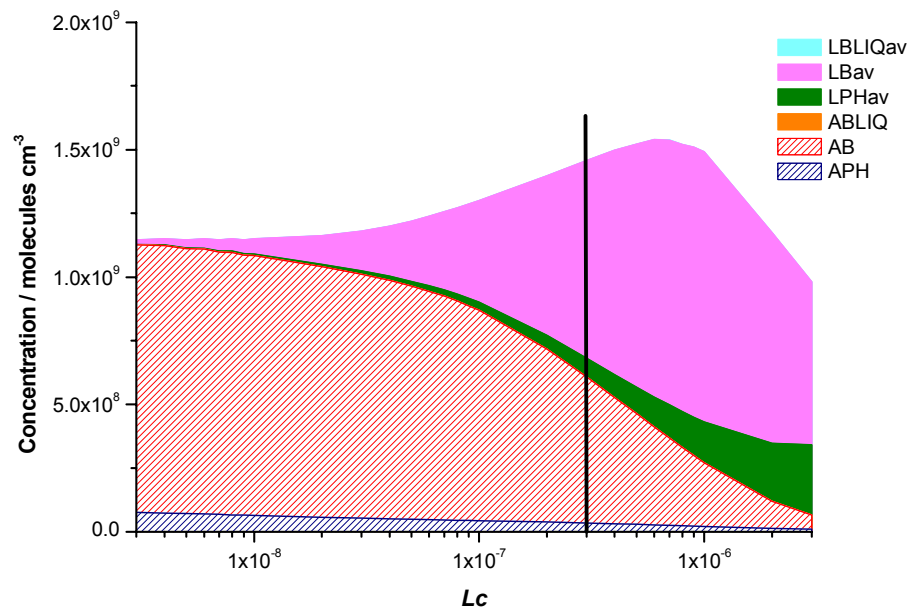


Fig. 3. The relative importance of the different nitration pathways at 278 K as a function of L_c .

Title Page

Abstract

Introduction

Conclusions

References

Tables

Figures

◀

▶

◀

▶

Back

Close

Full Screen / Esc

Print Version

Interactive Discussion

Pathways of nitrophenol formation using a multiphase model

M. R. Heal et al.

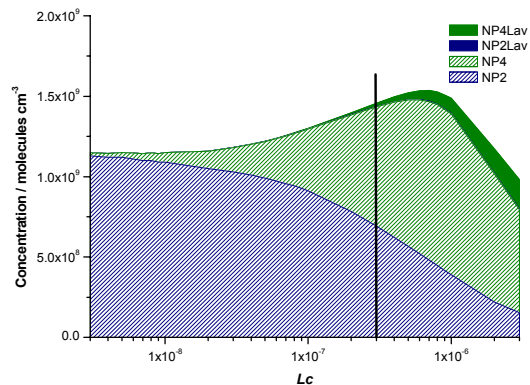
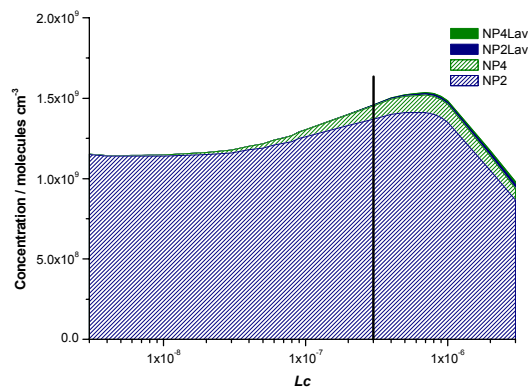


Fig. 4. The ratio of nitrophenols produced at 278 K as a function of L_c with the liquid phase reaction of NO_3 with phenol yielding (a) 90% 2-nitrophenol and 10% 4-nitrophenol and (b) 90% 4-nitrophenol and 10% 2-nitrophenol.

[Title Page](#)[Abstract](#)[Introduction](#)[Conclusions](#)[References](#)[Tables](#)[Figures](#)[◀](#)[▶](#)[◀](#)[▶](#)[Back](#)[Close](#)[Full Screen / Esc](#)[Print Version](#)[Interactive Discussion](#)

Pathways of nitrophenol formation using a multiphase model

M. R. Heal et al.

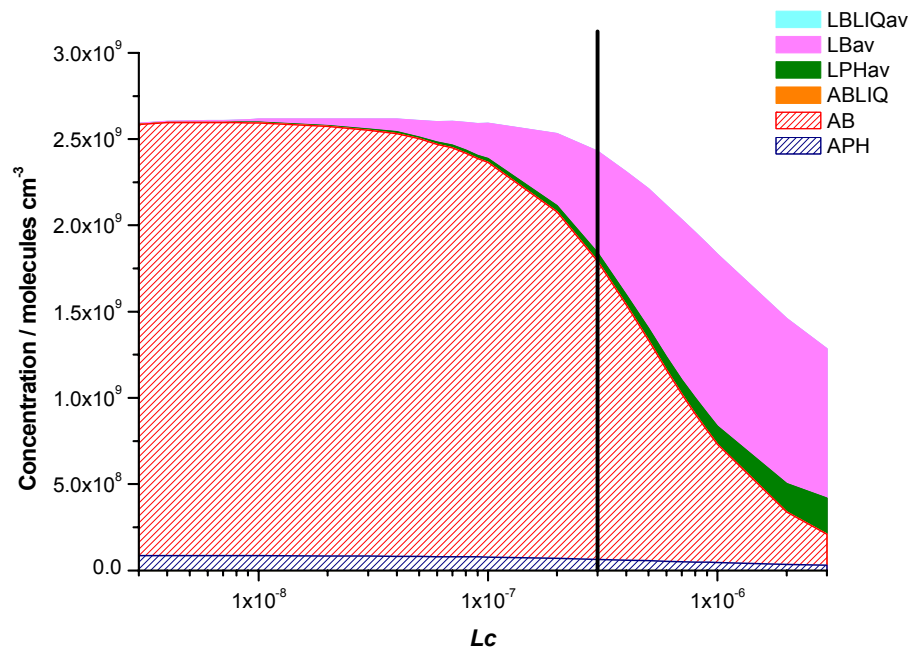


Fig. 5. The relative importance of the different nitration pathways at 298 K as a function of L_c .

Title Page

Abstract

Introduction

Conclusions

References

Tables

Figures

◀

▶

◀

▶

Back

Close

Full Screen / Esc

Print Version

Interactive Discussion

EGU

Pathways of nitrophenol formation using a multiphase model

M. R. Heal et al.

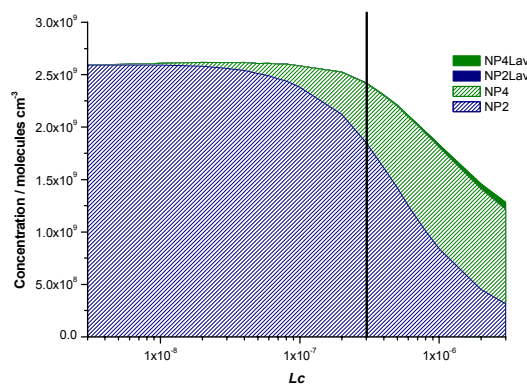
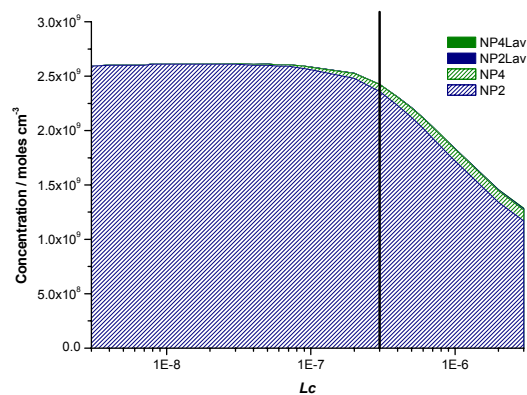


Fig. 6. The ratio of nitrophenols produced at 298 K as a function of L_c with the liquid phase reaction of NO_3 with phenol yielding (a) 90% 2-nitrophenol and 10% 4-nitrophenol and (b) 90% 4-nitrophenol and 10% 2-nitrophenol.

[Title Page](#)[Abstract](#)[Introduction](#)[Conclusions](#)[References](#)[Tables](#)[Figures](#)[◀](#)[▶](#)[◀](#)[▶](#)[Back](#)[Close](#)[Full Screen / Esc](#)[Print Version](#)[Interactive Discussion](#)

EGU

Pathways of nitrophenol formation using a multiphase model

M. R. Heal et al.

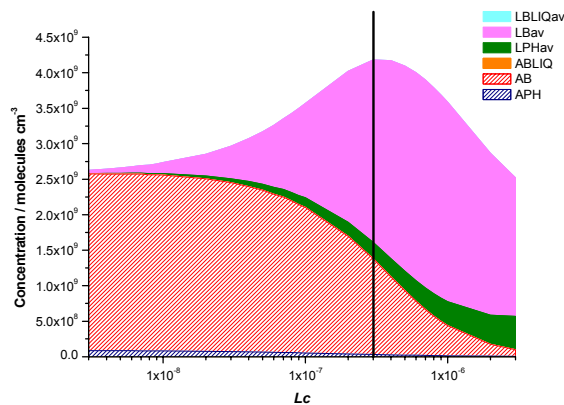
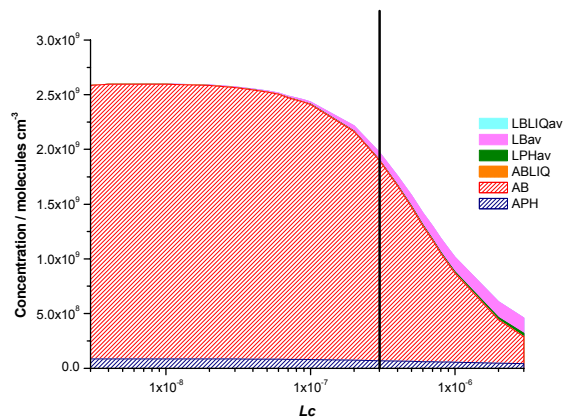


Fig. 7. The relative importance of the different nitration pathways at 298 K with the phenol + NO₃ liquid phase reaction rate coefficient set at (a) $1.8 \times 10^8 \text{ L mol}^{-1} \text{ s}^{-1}$ and (b) $1.8 \times 10^{10} \text{ L mol}^{-1} \text{ s}^{-1}$. (Compare with Fig. 5 for rate coefficient of $1.8 \times 10^9 \text{ L mol}^{-1} \text{ s}^{-1}$.)

[Title Page](#)
[Abstract](#)
[Introduction](#)
[Conclusions](#)
[References](#)
[Tables](#)
[Figures](#)
[◀](#)
[▶](#)
[◀](#)
[▶](#)
[Back](#)
[Close](#)
[Full Screen / Esc](#)
[Print Version](#)
[Interactive Discussion](#)

Pathways of nitrophenol formation using a multiphase model

M. R. Heal et al.

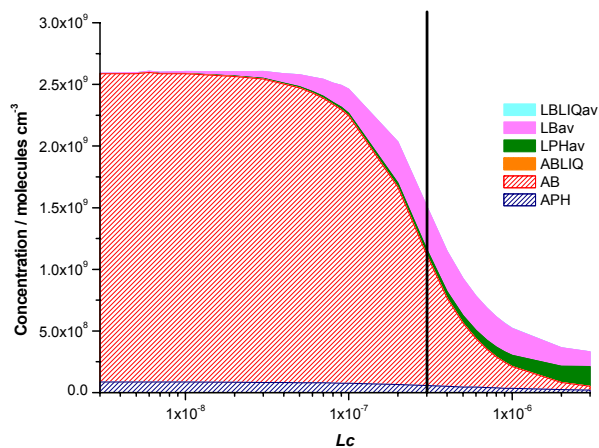
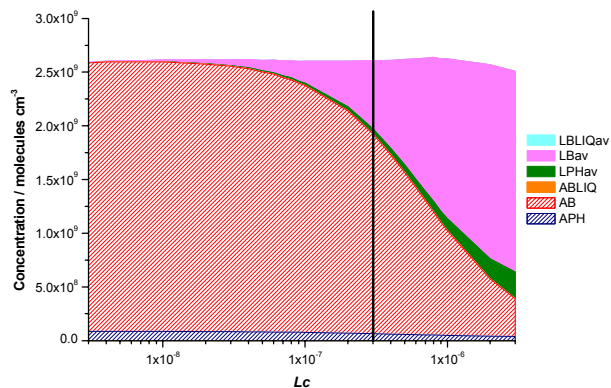


Fig. 8. The relative importance of the different nitration pathways at 298 K with the phenol + OH liquid phase reaction rate coefficient set at **(a)** $6.6 \times 10^8 \text{ L mol}^{-1} \text{ s}^{-1}$ and **(b)** $6.6 \times 10^{10} \text{ L mol}^{-1} \text{ s}^{-1}$. (Compare with Fig. 5 for rate coefficient of $6.6 \times 10^9 \text{ L mol}^{-1} \text{ s}^{-1}$.)

[Title Page](#)
[Abstract](#)
[Introduction](#)
[Conclusions](#)
[References](#)
[Tables](#)
[Figures](#)
[◀](#)
[▶](#)
[◀](#)
[▶](#)
[Back](#)
[Close](#)
[Full Screen / Esc](#)
[Print Version](#)
[Interactive Discussion](#)

Pathways of nitrophenol formation using a multiphase model

M. R. Heal et al.

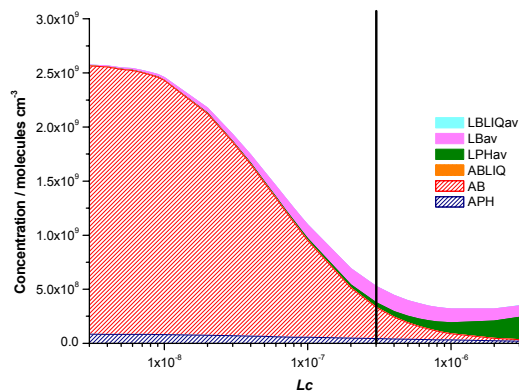
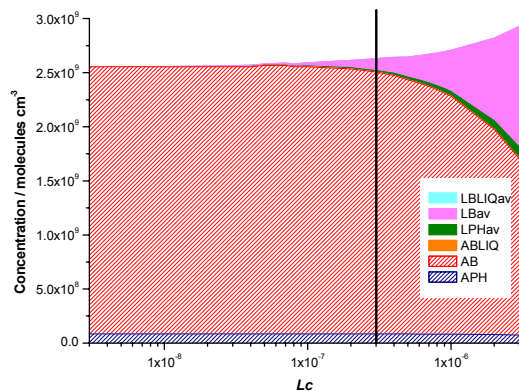


Fig. 9. The relative importance of the different nitration pathways at 298 K with monodisperse liquid droplet diameter of (a) 1×10^{-4} m and (b) 1×10^{-6} m. (Compare with Fig. 5 for diameter 1×10^{-5} m).

[Title Page](#)[Abstract](#)[Introduction](#)[Conclusions](#)[References](#)[Tables](#)[Figures](#)[◀](#)[▶](#)[◀](#)[▶](#)[Back](#)[Close](#)[Full Screen / Esc](#)[Print Version](#)[Interactive Discussion](#)